Co-processing of common plastics with pistachio hulls via hydrothermal liquefaction

Sukanya Hongthong, Sonia Raikova, Hannah Leese, Christopher J. Chuck*

Department of Chemical Engineering, University of Bath, Claverton down, Bath, BA2 7AY

*c.chuck@bath.ac.uk

Abstract

Mixed, wet, plastic streams containing food waste residues are being increasingly collected at point of use, but are extremely challenging to recycle and are therefore largely sent to landfill. While a challenging waste problem, this also represents an underutilised feedstock, which could be co-processed with biomass, increasing the scope of products, easing out seasonal variation in biomass production and increasing the production capacity of a traditional biorefinery. One promising method of biomass conversion is hydrothermal liquefaction (HTL), where lignocellulosic residues are broken down in water at high temperatures and pressures to produce a bio-crude oil, a solid residue and an aqueous fertiliser. In this study, the co-processing of common plastic waste with pistachio hulls was assessed to investigate the suitability of the HTL approach. The HTL of pistachio hulls was undertaken at 350 °C over 15 and 60 minutes, with four commonly used plastics: polyethylene, polypropylene, PET and nylon-6, in blends of up to 20 wt.% plastic to biomass. A novel FT-IR method was developed to estimate the conversion of plastics in the system, and the product phases were fully analysed. High yields of up to 35% bio-crude were achieved, and under optimal conditions, nylon-6 and PET were found to break down almost completely in the system. PET generated numerous products that distributed predominantly into the aqueous phase; the major decomposition product of nylon-6 was found to be the monomer ϵ-caprolactam, also largely partitioning into the aqueous phase. The polyolefins were less reactive; a limited degree of decomposition formed oxidised products, which distributed into the bio-crude phase. This result represents a highly promising method for waste plastic valorisation.

1. Introduction

Agricultural residues can be thermally processed through a variety of methods to produce bio-oils or bio-crudes that can be upgraded to chemicals and drop-in biofuels, or even combined in a traditional refinery (Elliott et al., 2015). For wet biomass, hydrothermal liquefaction (HTL) has been reported to be an economically viable route, which gives high biomass conversion yields and produce bio-crudes with favourable higher heating values (30–39 MJ kg^{-1}), lower oxygen contents (10–20 wt%), and a controllable water content (0–5 wt%) (Peterson et al., 2008). HTL avoids the need for drying the biomass, and instead uses pressurised vessels to keep water in the liquid phase; the pressure (10–25 MPa) is generated at moderate temperatures (290–350 °C) (Akhtar and Amin, 2011; Arturi et al., 2016; Bi et al., 2017; Demirbaş, 2001; Nazari et al., 2015; Tekin et al., 2014). At subcritical conditions, water behaves simultaneously as a solvent, reactant and catalyst for a number of biomass decomposition and repolymerization reactions. This results in a liquid bio-crude product, as an aqueous phase, a solid residue fraction, and a gaseous fraction.

Although the bulk of the early research on HTL has focused on microalgae (Biller et al., 2015), HTL of lignocellulosic materials is a promising alternative, especially if waste agricultural resources are used. To date, a number of studies have focused on HTL of lignocellulosic biomass. Typical bio-crude products from the HTL of lignocellulose includes aliphatic compounds, aromatics and phenolic derivatives, carboxylic acids, esters, and some nitrogenous compounds depending on the original protein level of the feedstock (Costanzo et al., 2016; Pedersen et al., 2016; Xiu et al., 2010). Hydrothermal liquefaction of lignocellulosic biomass is a well-known process and in depth modelling demonstrates significant energy and GHG savings in biofuel production when compared with fast pyrolysis routes (Tews et al., 2014). For example, a recent study has suggested that a fast pyrolysis process caused almost 50 % more global warming potential impact compared to the hydrothermal liquefaction process, due to both high energy demand in the drying process and high temperature operation of fast pyrolysis in the conversion of a lignocellusoic waste product. The assessment of other environmental impacts also indicated that the hydrothermal liquefaction operation is more environmentally benign compared to fast pyrolysis due to the reduced energy consumption (Chan et al., 2016).

Furthermore, the energy requirements for converting one tonne (1,000 kg) of Chlorella slurry via fast pyrolysis, microwave-assisted pyrolysis (MAP), and hydrothermal liquefaction (HTL) were

compared. Drying microalgae prior to pyrolysis by using a spray drying process with a 50% energy efficiency required an energy input of 4,107 MJ. The overall energy requirement of fast pyrolysis was found to be theoretically approximately 1.5x higher than that of HTL. The energy recovery ratios for fast pyrolysis, MAP, and HTL of microalgae were 78.7%, 57.2%, and 89.8%, respectively (Yang et al., 2017). Technoeconomic studies of the HTL of biomass show significant potential for commercialization of technology. Several lignocellulosic feedstocks have successfully been processed at high feed concentrations resulting in high energy recovery and carbon efficiencies. These have been demonstrated, that with a suitable processing size, to be economically viable (Elliott et al., 2015) (Zhu et al., 2014).

Pistachio processing waste is a lignocellulosic material with considerable potential for use as a biofuel feedstock (Taghizadeh-Alisaraei et al., 2017). A number of studies investigating the pyrolysis of pistachio waste have been published to date. Yields of between 20–33% bio-oil have been reported (Demiral et al., 2008) (Apaydin-Varol et al., 2007) (Pütün et al., 2007). Açıkalın et al. achieved a yield of over 50%, in a well-swept fixed bed reactor, though the bio-oil did have a comparatively low energy content of 19.5 MJ kg^{-1} (Açıkalın et al., 2012). To date, there have been no examples of liquefaction of this feedstock.

Processing of lignocellulosic wastes to biofuels is a promising step towards decreasing the environmental impacts of fuel production, but process sustainability can be further enhanced through the integration of bio-crude production with waste management, such as the co-liquefaction of biomass with plastic waste streams. The increasing volumes of plastic waste produced globally pose a significant threat to the environment and human health. In 2016, global plastic production reached 335 million tonnes (Association of Plastic Manufacturers Europe, 2017): a dramatic increase compared to 230 million tonnes produced in 2005 (Association of Plastic Manufacturers Europe, 2016). According to the World Bank, plastic waste accounts for 8–12% of total global municipal solid waste (MSW), estimated to increase to 9–13% of the MSW by 2025 (Bhada-Tata, March 2012). Although plastic waste in the UK is partially managed through recycling, vast quantities of plastics continue to accumulate in landfill (Wong et al., 2015) due to their extremely slow degradation rates (Bezergianni et al., 2017) (Demirbas et al., 2016). The most abundant elements in plastic wastes are carbon and hydrogen, and plastics typically have high H/C ratios (Karaca and Bolat, 2000) (Shui et al., 2011) (Shui et al., 2013) (Jongwon Kim, 1999), and correspondingly high energy contents. Therefore, the conversion of waste plastics to fuel

could be an elegant solution to both the issue of plastic waste and sustainable energy production.

In recent years, a number of studies on co-pyrolysis and co-liquefaction of biomass and plastics have been published (Uzoejinwa et al., 2018) (Wu et al., 2017). Thermochemical co-processing is possible, because there is an overlap between the temperature ranges of thermal decomposition for biomass and plastics (Jakab et al., 2000). It has been suggested that plastics, such as polyethylene (PE) or polypropylene (PP) can act as a source of hydrogen for biomass liquefaction to increase bio-crude yields and improve its fuel properties (Bhattacharya et al., 2009) (Cao et al., 2019; Fekhar et al., 2018) (Cao et al., 2019) However, to date, few reports have elaborated on the mechanisms of the interaction. Wu et al. reported the co-hydrothermal liquefaction of the microalga *Dunaliella tertiolecta* with polypropylene (Wu et al., 2017). Synergistic effects were observed for oil production, and the addition of PP led to improvements in the bio-oil quality, decreasing bio-crude acid content. Another study by Sørum et al. also demonstrated synergistic effects between PVC and pine wood sawdust during co-pyrolysis (Sørum et al., 2001). Seemingly, HCl released from the PVC under pyrolytic conditions behaved as an acid catalyst to promote dehydration of the biomass. However, under the same conditions, PE and PP did not have a substantial impact on pine wood sawdust pyrolysis. Wang et al. observed that co-liquefaction of Jingou lignite, wheat straw and plastic waste in sub-critical water gave optimal oil yields at a ratio of 5:4:1 (respectively), (Wang et al., 2014). Interestingly, they also found that the addition of tourmaline gave better oil yields and higher oil quality than when using conventional catalysts.

In this study, the co-liquefaction of pistachio hulls was undertaken for the first time and co-processed with several common plastics. Furthermore, the study aimed to elucidate the effect of plastic co-liquefaction of pistachio hulls on product distribution, yields, and product chemical compositions. PE, PET, PP, and nylon-6, and mixtures of the above, were used in this study.

2. Materials and methods

2.1 Materials

Pistachio hull was selected as a biomass feedstock representative of mixed food waste, and blended in varying ratios with polyethylene (PE), polyethylene terephthalate (PET), polypropylene (PP) and nylon-6 (hereafter referred to as “nylon”). Pistachio hull biomass (2–5

mm particle size) was obtained as a waste material after pistachio processing from the Wonderful Company (USA). PE, PET, PP and nylon were obtained from Sigma-Aldrich and ground using a commercial food blender to a particle size of <350 µm prior to use. Ultimate analysis was conducted following ASTM D5291 to determine carbon, hydrogen and oxygen. The high heating value of dry pistachio hull was 17.46 (MJ kg^{-1}) which was measured following ASTM E711. The biomass composition is given in the supporting information.

2.2 Hydrothermal liquefaction of co-liquefaction of pistachio hull

Co-hydrothermal liquefaction of pistachio hulls with plastics was carried out in a 50 mL stainless steel batch reactor. The reactor was equipped with a pressure gauge and pressure relief valve, and a needle valve to release gaseous products. The temperature was monitored using a thermocouple connected to data logging software. In a typical experiment, the reactor was loaded with a total of 3 g material (pistachio hull blended with PE, PP, PET, nylon, or a mix of the four plastics). Biomass: plastic weight ratios examined were 100:0, 90:10 and 80:20. The 90:10 ratio experiments contained 2.7 g of biomass and 0.3 g of either PE, PP, PET or nylon. For the 80:20 weight ratio, the experiments contained 2.4 g of biomass and 0.6 g of either PE, PP, PET, or nylon. The feedstock was mixed with 15 g of distilled water to form a slurry. The reactor was sealed and loaded into a preheated furnace to either 500°C or 700°C. The reactor was held in the furnace until the temperature reached 350 °C, 60 and 15 min, respectively. Upon reaching the desired temperature, the reactor was removed from the furnace and allowed to cool to room temperature. Each experiment was repeated three times to determine experimental error.

2.3 Separation of liquefied product

After cooling, gaseous products were released via the needle valve into an inverted, water-filled measuring cylinder to measure total gas volume. Gas phase yield was calculated from volume using the ideal gas law. The reactor contents were filtered through a filter paper to separate the aqueous phase from the water-insoluble fraction (consisting of the bio-crude and bio-char). The solid-liquid mixture remaining on the filter paper was washed repeatedly with chloroform until the solvent ran clear. The chloroform was removed using a rotary evaporator at 35 °C for 2 hours to isolate the bio-crude. The solids were oven-dried overnight at 60°C to determine the solid phase product yield. An aliquot of the aqueous phase products was dried overnight at 60°C to

determine the yield of non-volatile organics and inorganics in the aqueous phase, designated as "aqueous phase residue".

2.4 Yield of product

The yields of each product phase were calculated as mass percentage on a dry basis. Bio-crude was calculated from mass left after remove residual solvent via rotary evaporation. Bio-crude yield was determined using the following equation:

$$yield_{bio-crude} = \frac{mass\ bio-crude\ (g)}{mass\ dry\ biomass\ (g) + mass\ plastic(g)} \times 100 \quad (1)$$

The char yield was calculated from the collected char mass on the filter paper after letting it dry in an oven at 60℃. Solid yield was determined using the following equation:

$$yields_{solid} = \frac{mass\ solid\ phase\ (g)}{mass\ dry\ biomass\ (g) + mass\ plastic\ (g)} \times 100 \quad (2)$$

Gas volume was calculated according to literature precedent, by using the ideal gas law and assuming that the gas was completely CO_2 (Raikova et al., 2016).

$$yield_{gas} = \frac{(gas\ volume \times 1.789 \times 10^{-3})}{mass\ dry\ biomass\ (g) + mass\ plastic\ (g)} \times 100 \quad (3)$$

The solid yield in the aqueous phase was calculated by taking a 2.0 g aliquot of the phase and drying at 60 ℃. Aqueous phase residue yield was determined using the following equation:

$$yield_{aqueous\ residue} = \frac{mass\ of\ bio-crude\ oil\ (g)}{mass\ dry\ biomass\ (g) + mass\ plastic\ (g)} \times 100 \quad (4)$$

The overall mass balance of the reaction was calculated as follows:

$$mass\ balance\ (\%) = solid\ (\%) + bio\text{-}crude\ (\%) + aqueous\ residue\ (\%) + gas\ (\%) \quad (5)$$

2.5 Characterisation of HTL products

The chemical composition of the volatile fraction of the bio-crude was investigated using an Agilent Technologies 7890A GC system fitted with a 30 m × 250 µm × 0.25 µm HP5-MS column, coupled to a 5975C inert MSD. Samples were dissolved in THF, and helium (1.2 mL min^{-1}) was used as the carrier gas. Initial oven temperature was set to 50°C, increasing to 250 °C at 10 °C min^{-1}. Initial identification of compounds was performed using the NIST mass spectral database.

Solid phase products were analysed using FTIR. Spectra were recorded on a Thermo Scientific Nicolet iS5 FTIR spectrometer in the wavenumber range between 4000–600 cm^{-1}. FTIR was used to assess the level of unreacted plastic remaining in the solid phase products as a proxy for the extent of plastic conversion. Calibration curves were developed by mixing known amounts of bio-char from the HTL of pure pistachio biomass with known amounts of plastics and grinding finely in a mortar and pestle to ensure a homogeneous blend. The blended samples were analysed by FTIR, and two characteristic absorbance's were selected for each plastic/biomass combination, one unique to the plastic, and another unique to the biomass component. The ratio of the two absorbance's was calculated as described in the study of Lao and Li (Lao and li, 2014), and used to create a calibration curve, against which the samples of bio-char produced experimentally were assessed. Each bio-char sample was analysed in triplicate; average values of absorbance ratio were used to calculate conversion. Further information is given in the supporting information.

2.6 Elemental analysis, carbon and energy recoveries

Elemental analysis (carbon, hydrogen and nitrogen content) of the biomass feedstock and products was carried out externally at London Metropolitan University on a Carlo Erba Flash 2000 Elemental Analyser. Oxygen content was determined by difference, assuming negligible sulphur in the products.

$$O\ (wt\%) = 100 - C - H - N\ (wt\%) \quad (6)$$

The higher heating values (HHV) of the biomass, bio-char and bio-crude were calculated using the Dulong formula, where C, H, and N are the weight percentages of each element:

$$HHV\ (MJ\ kg^{-1}) = 0.3383C + 1.422\left(H - \left(\frac{O}{8}\right)\right) \quad (7)$$

Energy recovery in each product phase was calculated as follows:

$$Enery\ recovery\ (\%) = \frac{HHV\ product\ (\%) \times Mass\ of\ product\ (\%)}{HHV\ of\ feedstock\ (\%)} \quad (8)$$

3. Results and Discussion

3.1 Effect of waste plastic contents on bio-crude yields and mass balance

Initially, the influence of the ratio between pistachio hull waste and plastic in the HTL feedstock on the distribution of product phases was investigated. HTL was carried out at 350 °C for 15 minutes, based on previously reported optimal conditions (Raikova et al., 2019). Mass balances are shown in Figure 1a where product yields were calculated on the basis of total feedstock (biomass and plastic) input.

In general, co-liquefaction with plastics resulted in an increase in overall bio-char yields relative to the HTL of pistachio hulls alone. The most significant impact was observed for co-liquefaction with PE, with a substantial increase in bio-char production from 22.1% to 35.6 % at a 10 wt.% blend, and from 22.1% to 40.7 % at a 20 wt.% blend. On the addition of PE, the yield of gas phase product increased slightly from 15.9 % for pure pistachio to 17.8 % for a 10 wt.% PE blend, but decreased slightly for a 20 wt.% PE blend to 15.1 %. Blending feedstocks with polyethylene was found to deplete bio-crude yields substantially, with yields decreasing from 34.1 % to 20.4 % for a 10 wt.% PE blend, but increasing somewhat to 26.8 % for 20 wt.% PE. The aqueous phase residue yield was not significantly impacted by co-liquefaction with PE and only a slight yield increase of 1.0–1.5 % was observed for 10 wt.% and 20 wt.% PE blends respectively.

For PP, higher yields of bio-crude were obtained for the 10 wt.% PP blend, whereas slight decreases were seen for the 20 wt.% PP blend (bio-crude yields of 36.3 % and 30.7 % respectively). The addition of PP also had a significant effect on bio-char production – bio-char yield increased from 22.1% to 30.1 % for the 10 wt.% PP blend, and rose further to 40.3 % for the 20 wt.% PP blend. The gas phase product yields obtained from both the 10 wt.% and 20 wt.% PP blends were similar to those obtained for HTL of pure pistachio. Co-liquefaction with PP contributed to a modest increase in aqueous phase residue production – (from 8.3% to 10 % for

10 wt.% PP loading and up to 9.6 % for the 20 wt.% PP loading). The majority of the PE and PP were recovered in the solid phase products.

For PET, the gas phase products were not strongly impacted by co-liquefaction, with 16.2 % gas phase produced at 10 wt.% PET, although this dropped to 13.2 % for the 20 wt.% PET blend. Bio-crude yields obtained on PET co-liquefaction showed a slight increase compared to HTL of pure pistachio (bio-crude increased by 0.6 % for the 10 wt.% PET blend to 34.6 %, and remained almost unchanged for the 20 wt.% blend). In addition, PET was found to increase bio-char production to 24.2 % and 37.8 % for the 10 wt.% and 20 wt.% PET blend. As for PE and PP, aqueous phase residue obtained from PET blend was again not strongly affected, with a slight increase of 1.7 % and 1 % observed for the 10 wt.% and 20 wt.% PET blend.

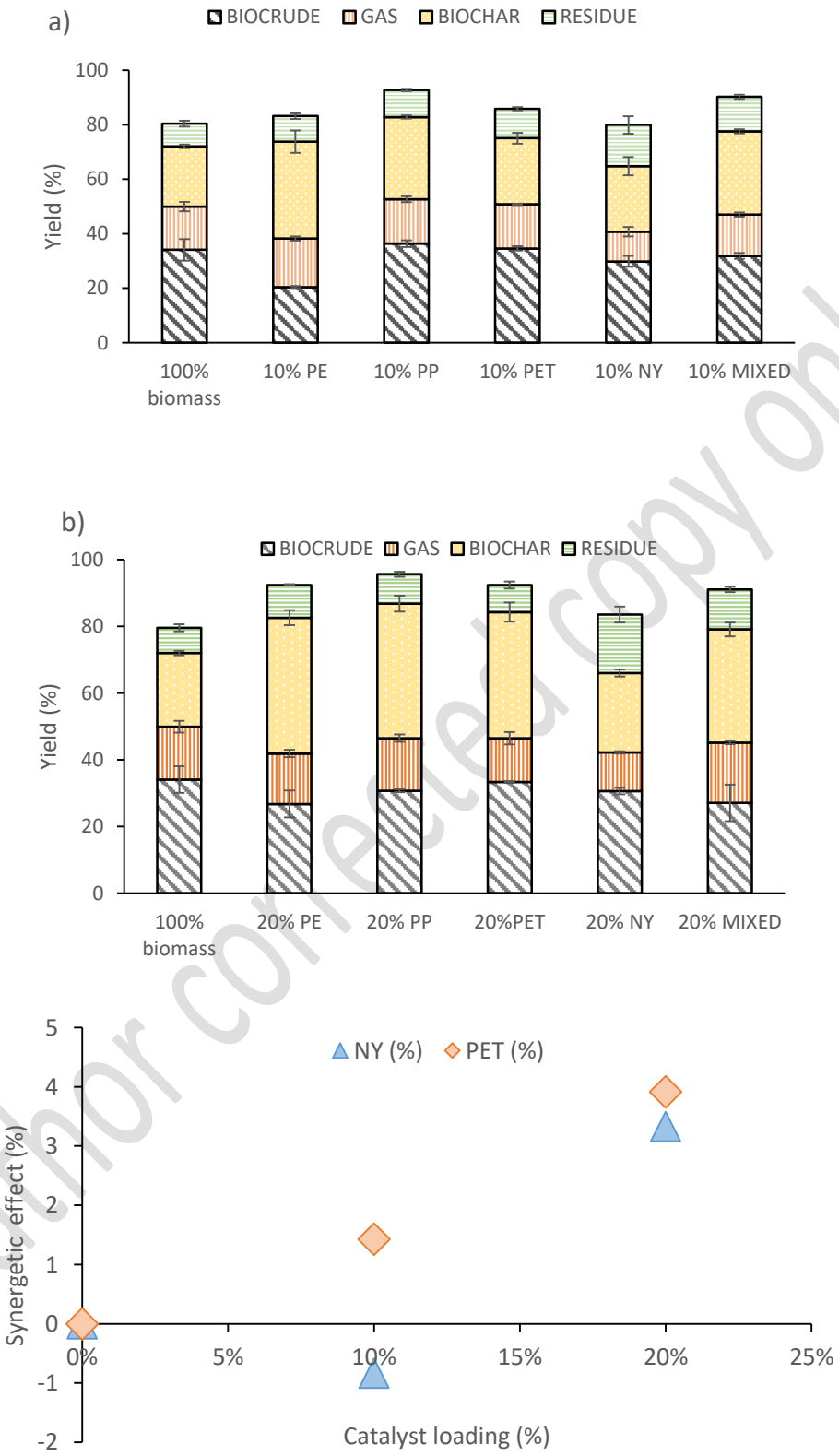

Figure 1 a) Mass balance of HTL product from liquefaction of pistachio hull with PE, PP, PET, NY, and plastic mixture at (a) 10 wt.%, and (b) 20 wt.% of plastic blend loading. **b)** Synergistic

effect on bio-crude yields from co-liquefaction of pistachio hull/PET and pistachio/Nylon blends (PET = polyethylene terephthalate, NY = Nylon)

In contrast with the other plastics, the increase in bio-char production was much smaller for the co-liquefaction of pistachio hull with nylon (24.1 % and 23.8 % bio-char for 10 wt.% and 20 wt.% NY, compared to 22.1 % for the liquefaction of pure pistachio hull). Bio-crude yields obtained for the nylon blends were 30.0 % for the 10 wt.% NY blend, whilst the 20 wt.% NY blend gave a similar yield of 30.1 %. Gas phase product yields decreased from 15.9 % for pure pistachio hull to 11.0 % at the 10 wt.% NY blend level and 11.6 % for the 20 wt.% NY blend. Residue from the aqueous phase increased substantially from 8.3 % for pure pistachio hull HTL to 15.1 % and 17.5 % for 10 wt.% and 20 wt.% nylon blends, respectively.

Co-liquefaction of pistachio hull with a mix of the plastics in equal proportions increased bio-char production substantially to 30.6 % and 33.9 %, respectively, for 10 wt.% and 20 wt.% blends, whilst bio-crude yields decreased to 31.9 % for the 10wt% plastic loading, and subsequently to 27.1 % for the 20wt% loading. Gas yields were not strongly affected. Aqueous phase residue yields obtained from HTL of pistachio hulls with the plastic mix showed a slight increase compared to pure pistachio hulls, rising from 8.3 % to 12.6 % and 13.3 % for 10 wt.% and 20 wt.% blends, respectively.

Co-processing with plastics does not appear to have a significant benefit in terms of bio-crude oil production from pistachio hull. Bio-crude oil yields obtained from co-liquefaction at 10 wt.% and 20 wt.% plastic blends were similar to those produced from pistachio hull waste alone for PP, PET and nylon, and depleted significantly for PE. With PET and NY there is a potential interaction between the biomass and the plastics where the biomass could synergistically aid the breakdown of plastic. The synergistic effect of the interaction between biomass and plastics can be determined by the equation 9 below:

$$Synergistic\ effect = Ybiocrude - (Xpistachio\ \times Ypistachio + (1 - Xplastic) \times Yplastic) \quad (9)$$

where, $Y_{biocrude}$ is the yield of bio-crude obtained in experiment, $X_{pistachio}$ and $X_{plastic}$ are the mass fraction of pistachio and plastics in the total reaction mixture, $Y_{pistachio}$ is the bio-crude yield of pure pistachio, and $Y_{plastic}$ is the bio-crude yield of pure plastic.

As PE and PP do not react under these conditions without biomass present, the synergistic effect was only calculated for the co-liquefaction of PET/biomass and nylon/biomass blends. Overall the presence of biomass enhances the conversion of the plastic in the liquefaction process, and a positive correlation was observed for the total bio-crude yield, with the exception of the 10%wt nylon blend (Figure 1b). The positive effect of a synergy between biomass and PET, increasing the bio-oil yield was also observed by Çepelioğullar and Pütün, during co-pyrolysis of hazelnut shells with PET (Çepelioğullar and Pütün, 2013).

3.2 Bio-char composition and properties

To determine the fate of the plastics, the bio-char was analysed by elemental analysis and FT-IR. The elemental composition of the bio-char produced through the co-liquefaction is presented in Figure 2. Overall, there was substantial variation in the elemental composition of the bio-chars. For example, the carbon content ranged from 50.5–75.5 %, nitrogen content ranged between 1.3–3.9 %, hydrogen contents between 3.6–9.3 % and oxygen contents of 17.1–44.0 % were observed. Co-liquefaction with PET caused the most substantial decrease in C and increase in O content in bio-chars (from 61.2 % C and 30.1 % O for pure pistachio bio-char, to 50.5 % C and 44 % O obtained for bio-char from co-liquefaction of pistachio with 20 wt.% PET). Co-liquefaction with PP contributed to an increase in C content (71.9 % and 72.3 % C for 10 wt.% and 20 wt.% PP blends, respectively). The additional PE bio-char had the highest carbon content and the lowest nitrogen (75.5 % and 1.3 %, respectively). This is suggestive that the PE and PP is not breaking down and rather distributing into the char.

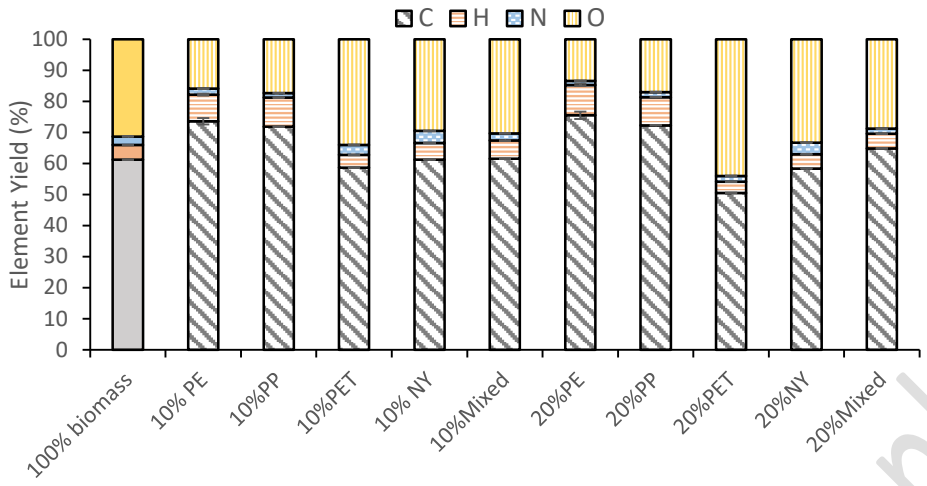

Figure 2 Elemental composition (determined by elemental analysis) of the bio-char of different plastic contents 10 wt.% and 20 wt.% of PE, PP, PET, NY and plastic mixture.

The heating value (HHV) is commonly used to describe the energy content of any fuel (Qian et al., 2013). The bio-char produced in the HTL reaction is also suitable for combustion and as such the HHV of the bio-chars produced were calculated (Figure 3a). While the bio-char from pistachio hull had a very similar energy content to those produced from the nylon and PET reactions, the bio-char produced from the PE and PP liquefactions was extremely high with up to 37 MJ kg^{-1} observed. This suggests that the majority of the polyolefins are not reacting, and rather remaining in the bio-char increasing the HHV.

One method of assessing the suitability of bio-chars as a solid fuel is to determine and compare the elemental ratios of H/C and O/C through a Van Krevelen diagram (Van Krevelen, 1950). The H/C and O/C ratios also give an indication of the structural transformation (Wang et al., 2015) and surface hydrophilicity of bio-char (Tan et al., 2015). In this study, similar to the HHV, an increase of H/C ratios was found for the presence of PE and PP blends compared to pure pistachio, and a slight increase in the H/C ratios from 0.92 to 1.09 and 1.08 for the presence of 20 wt.% PP and PE blends, respectively. In the contrast, the H/C ratio was much smaller for pistachio with PET. The H/C ratio obtained for the bio-char from nylon blends were 0.74 and 0.66 for 10 wt.% and 20 wt.% nylon blends.

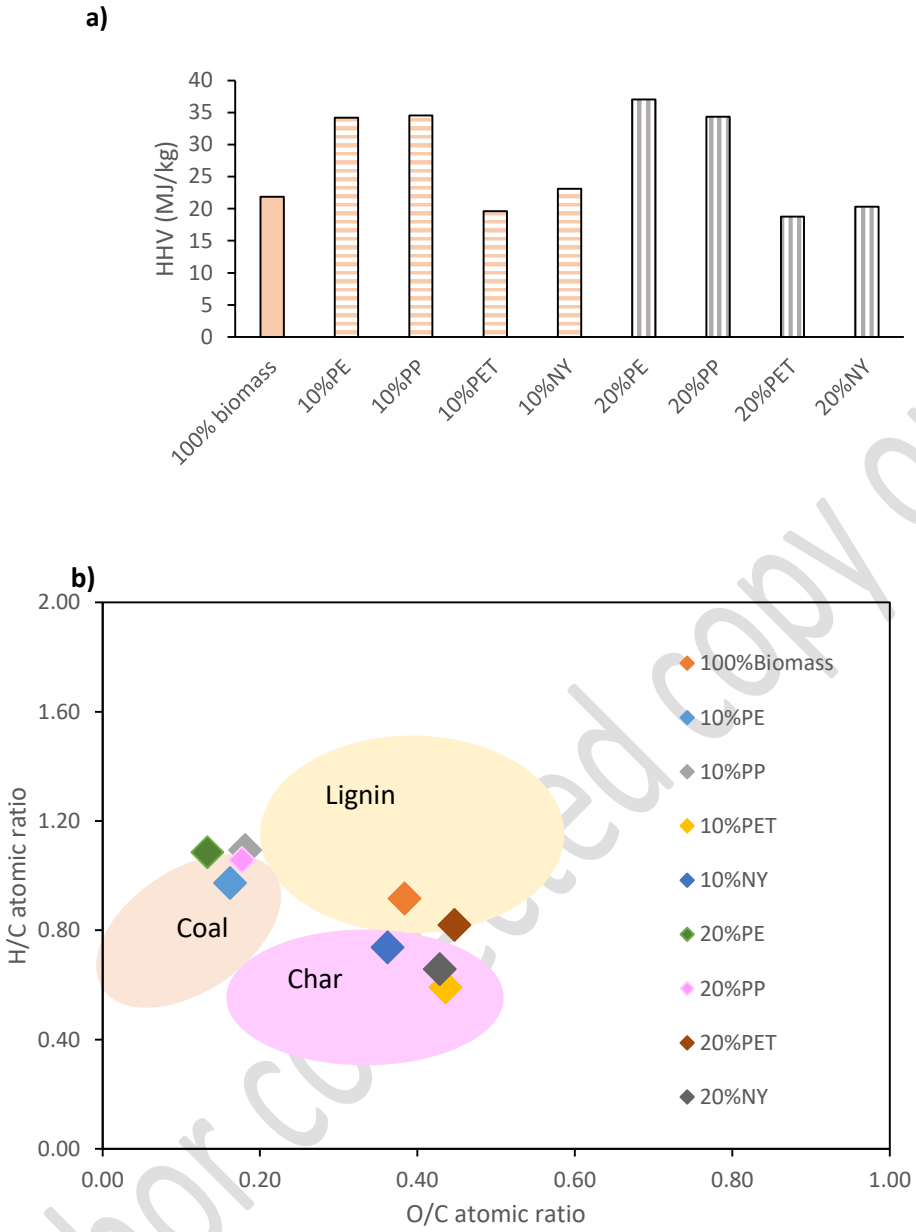

Figure 3 a) Bio-char heating value of the bio-char of different plastic contents 10 wt.% and 20 wt.% of PE, PP, PET, and NY. **b)** Van Krevelen diagram with H:C and O: molar ratio for co-liquefaction of biomass with plastics char, coal, and lignin (Kookana et al., 2011)

For the O/C ratio (the degree of polarity), the additional PET has the highest O/C ratio (0.45 and 0.44 for10 wt.% and 20 wt.% PET blends). Co-liquefaction of nylon contributed to an increase 0.43 for 20 wt.% nylon but slight decrease to 0.36 for 10 wt.% nylon blend. The smallest O/C ratio was found in the additional PE (0.16 and 0.13 for 10 wt.% and 20 wt.% PE blends). Similarly, 0.18 C/O ratio was observed for 10 wt.% and 20 wt.% PP blends. The H/C and O/C ratios for the bio-chars in this study were plotted and compared to typical solid heating fuels (Figure 3b).

A lower H/C and O/H ratio have been assumed to be due to a greater the degree of aromaticity and stability (Kookana et al., 2011). The positions of the bio-char from PE and PP were similar to coal, and were presumably increased by a large level of unreacted plastic in the solid residue. For the bio-char from biomass/PET and biomass/nylon were found ranging in between lignin and nature char, this indicates a higher level of conversion in these reactions.

3.3 Identification of major functional groups in bio-char

Hydrothermal conversion of biomass produces bio-char as one of the major products, although HTL bio-char is structurally different to bio-char derived from high-temperature pyrolysis (Hu et al., 2018). For example, HTL bio-char tends to have a higher abundance of oxygen-containing functional groups (Liu et al., 2010). In order to achieve a better understanding of the effect of plastics on pistachio hull HTL, bio-chars were analysed using FT-IR to identify the key functional groups present.

The FT-IR spectra of bio-char from HTL of pure pistachio contained strong absorption bands at 2800–3300 cm^{-1}, attributable to C–H stretching vibrations from methyl and methylene-containing organic compounds. An absorbance attributed to alkane bending is seen at 1066–1145 cm^{-1}. The presence of esters and acids in the spectra is evidenced by the strong C=O absorbance at 1800–2000 cm^{-1}. The absorption peak observed around 1612 cm^{-1} can be assigned to aromatic rings in lignin and thus verified to the presence of lignin in bio-char (Konsolakis et al., 2015). A vibration at 1570 cm^{-1} and 898 cm^{-1} can be attributed to the presence of aromatic rings, likely arising from asphaltenic materials in the bio-char (Wang and Griffiths, 1985) (Lua and Yang, 2004). A similar observation was also reported for the pyrolysis of pistachio shell (Açıkalın et al., 2012; Apaydin-Varol et al., 2007) and green fabrication of Cu/pistachio shell nanocomposite (Taghizadeh and Rad-Moghadam, 2018).

For bio-char from co-liquefaction of pistachio hull with PE, peaks of moderate intensity were observed at 2936, 1593, 1267 cm^{-1}, similar to those obtained for bio-char from HTL of pure pistachio hull. However, sharp peaks at 2850 and 2920 cm^{-1} are also present, which are not observed for pure pistachio hull bio-char, attributable to C–H bonds (Figure 4a). In addition, peaks were observed at 1451 and 1376 cm^{-1}, which were also seen in the FT-IR specta of pure

PE, but not in the spectra of the bio-char from pistachio hull liquefaction. These findings suggest the presence of unreacted polyethylene in the HTL char.

On comparing the spectra of the bio-char from the HTL of pistachio hull, the bio-char from pistachio hull co-liquefaction with PP, and pure unreacted PP, absorbance attributable to C–H bond stretching vibrations at 2920 cm^{-1} and 2849 cm^{-1} are present in the co-processed samples and the pure PP, which are not seen for bio-char from pure pistachio hulls (Figure 4b). Additionally, with increasing PP loading in the blended samples, peaks at 1365 and 1420 cm^{-1} attributable to alkane C–H bending sharpen, suggesting the presence of increasing amounts of unreacted PP.

For bio-char produced from blended pistachio hull and PET, a number of peaks at similar wavenumbers to pure PET were observed (2920 cm^{-1}, 1017 cm^{-1}, 872 cm^{-1}), suggesting the presence of some unreacted plastic. However, a number of additional peaks unique to the blended pistachio/PET bio-char, and not present in either pure PET or bio-char from pure pistachio, were also observed at 820, 1400 and 1575 cm^{-1}: these are attributed to C–H, O–H and C=C bonds. The appearance of new absorbance peaks can be taken as evidence of reactions occurring between the biomass and PET under HTL conditions, and the formation of new compounds (Figure 4c).

In contrast, the FT-IR spectra of bio-char from the HTL of pistachio hulls blended with nylon were almost identical to the spectrum of pure pistachio hull bio-char (weak absorbance at 1570 cm^{-1}, 1249 cm^{-1}, 1068 cm^{-1} and 720 cm^{-1}, corresponding to O–H stretching vibrations and aromatic C=C bonds (Figure 4d). The presence of nylon co-feedstock in HTL reactions did not appear to change to composition of the bio-char, suggesting that nylon reacted more completely, forming more soluble products than the other three plastics examined.

The FTIR spectra of the char are high similar however, those produced from the co-liquefaction with PE and PP blends show a far stronger absorbance at ~2800-3000 cm^{-1} suggestive of an aliphatic functional group (Chen et al., 2008). These intensive peaks, coupled to the enhanced C and H contents, as well as HHV of the char strongly suggest unreacted polymer. In contrast, the intensity of these peaks decreased substantially in the char produced from the PET and nylon co-

liquefaction studies. So much so, that the FTIR spectra of the biochar produced from the nylon blends closely resembles the char produced from pure pistachio hull. These results suggest that during co-liquefaction of pistachio and nylon, there is synergetic interaction between the two components improving decomposition. The complete decomposition of nylon is in agreement with another previous study of the co-liquefaction with macroalgae (Raikova et al., 2019). The most resistant polymer to decomposition was PE and this is presumably due to the to the high activation energy needed to decompose the polymer, the instability of the potential secondary products and to diffusion limitation caused by PE melted during the HTL process (Burra and Gupta, 2018).

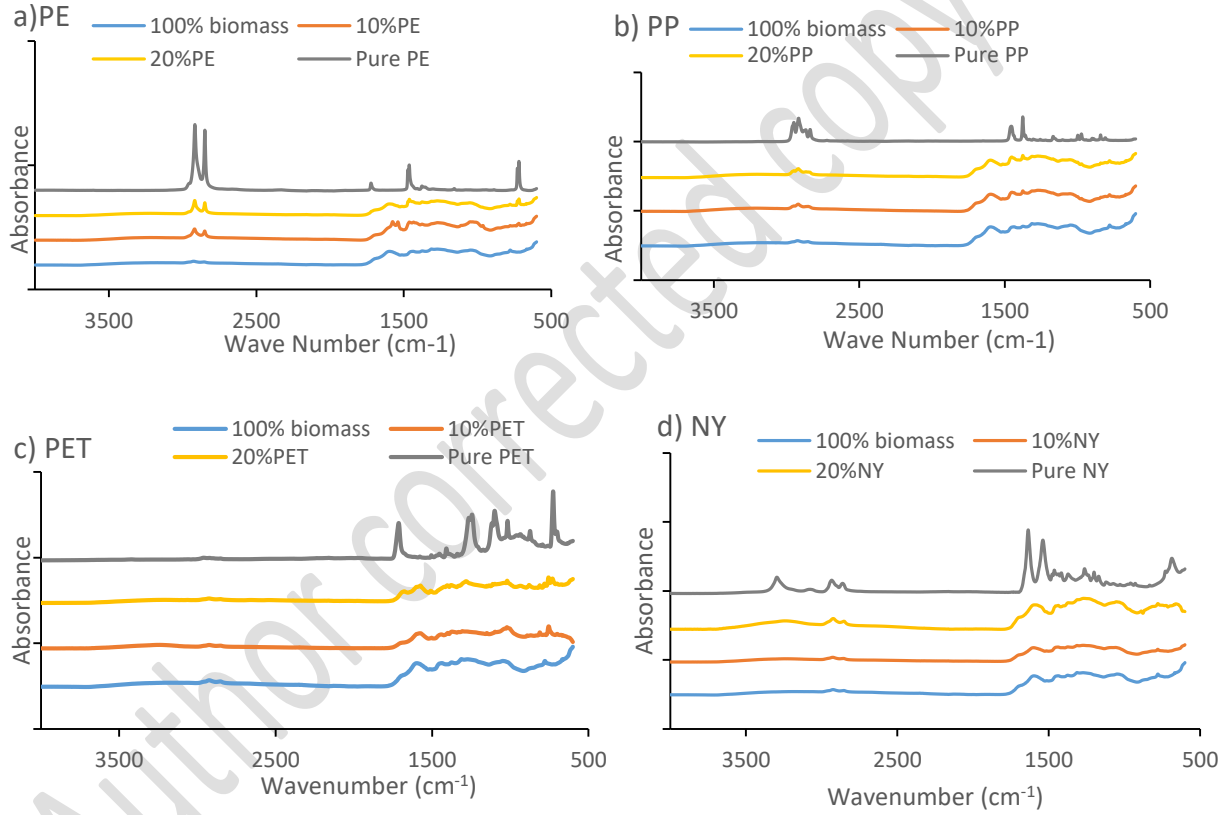

Figure 4 FTIR of pure plastics and solid phase from hydrothermal co-liquefaction of pistachio hull with (a) polyethylene, (b) polypropylene, (c) polyethylene terephthalate, and (d) nylon.

3.4 Quantification of unreacted plastic in bio-char

The presence of plastics alongside pistachio hull biomass had an effect on the yields and composition of the four product phases. It is important to be able to quantitatively understand

what proportion of the plastic remained unconverted in the HTL reaction, and how plastic degradation products are distributed between the four product phases. Co-liquefaction of pistachio hulls with all four plastics enhanced the partitioning of material to the bio-char phase. This may be attributable to a number of factors: the presence of unreacted plastics, plastics partially or entirely converted to new solid-phase product molecules, biomass-derived solids converted to bio-char in higher quantities in the presence of plastic or a combination of the above. By identifying the proportion of unreacted plastics in the bio-char phase, it is possible to assess the degree of plastic conversion. Fourier transform infrared (FTIR) spectroscopy has played an important role in quantitative analysis of mixed solid materials in a number of studies, and can be a simple and inexpensive technique for determining plastic content in biogenic samples.

Chen et al. demonstrated quantitative determination of clay minerals, quartz and carbonates, as well as organic matter in shale, using KBr-FTIR spectroscopy (Chen et al., 2014). Pandey and Pitman used FTIR to investigate the lignin content in wood and wood decayed by the brown-rot fungus *Coniophora puteana,* by identifying characteristic FTIR absorbance peaks for lignin and wood, and using the ratio of peak intensities to determine lignin content (Pandey and Pitman, 2004). Lao et al. demonstrated that FTIR could be used to quantify biomass in wood-plastic composites. FTIR was used to analyse the wood samples and plastics independently, and peaks which were unique to the biomass and plastic components were identified (Lao and li, 2014). Taking a number of composites with different biomass contents, the peak ratios of the signature biomass and plastic peaks were calculated, and univariate regression was used to generate equations to predict biomass content in composites. Another study of wood-plastic composites by Stark and Matuana (Stark and Matuana, 2007) used Attenuated Total Reflectance Fourier Transform Infrared (ATR-FTIR) spectroscopy combined with principal component analysis to classify wood-plastic composites species.

In this study, the conversion of plastics were estimated by plotting calibration curves of known amounts of the plastics with bio-char generated from the reaction which contained only pistachio hull. Calibration curves were created for each plastic/biomass combination (polyethylene/pistachio hull, polypropylene/pistachio hull, polyethylene terephthalate/pistachio hull, nylon/pistachio hull) by mixing bio-char from HTL of pure pistachio hull with plastics at a

range of known concentrations. Calibration curves and further information are provided in the Supplementary Information (Table S3–S6, and Figure S1–S4).

The content of unreacted plastics in the bio-char phase can be used to determine the overall conversion, which includes plastics converted to water-soluble material in the aqueous phase, as well as bio-crude, volatile gas-phase products and plastic-derived materials in the solid bio-char phase that have undergone reactions to form new molecules (although it excludes polymer chains that may have undergone reactions and lost several repeat units, but remained otherwise unchanged in the bulk of the chain).

$$Conversion\ (\%) = \frac{unconverted\ plastic\ in\ bio{-}char\ (\%) \times\ bio{-}char\ yield\ (g)}{plastic\ in\ feedstock\ (g)} \qquad (10)$$

Conversions of the bulk plastic are presented in Figure 5. Nylon demonstrated the highest overall conversion through HTL (84 %); PET conversion was also high (53 %). In contrast, polyethylene and polypropylene were highly resistant to degradation. For polyethylene, only 17 % was converted into HTL products at a 10 wt.% blend, but no conversion was observed for the 20 wt.% blend. For polypropylene, approximately 9 % was converted at 20 wt.% blend level, although the 10 wt.% blend showed little reactivity. Out of all the plastics examined, PE blends were remarkably resistant to degradation. Co-liquefaction of PE blends is may attributed to diffusion limitation caused by PE melted during HTL process and increase in the stability of its decomposed (Burra and Gupta, 2018).

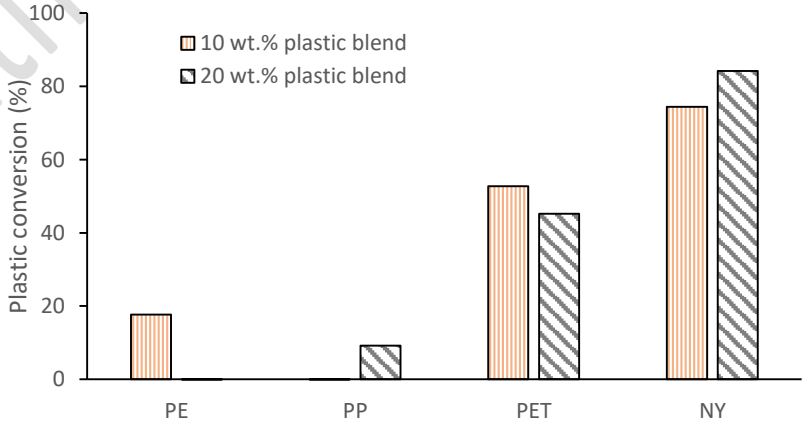

Figure 5 Extent of plastic conversion under HTL conditions

3.5 Bio-crude elemental composition

The main product produced from the HTL conversion was the bio-crude that can be converted into an array of platform chemicals and biofuels (Biller et al., 2015). Elemental composition of the bio-crude produced from co-liquefaction of pistachio hulls with plastics did not change substantially relative to bio-crude from pure pistachio hulls (Figure 6a). Carbon content increased slightly for co-liquefaction with PE and PET, although small reductions were seen for co-liquefaction with PP and NY. Nitrogen content slightly increased with the addition of PE and nylon, which gave rise to increases in bio-crude N from 1.73 % for pure pistachio hull bio-crude to 2.18 % and 2.43 % for 10 wt.% and 20 wt.% PE blend loading and increased to a maximum of 3.47 % for a 20 wt.% nylon blend level. Oxygen levels were relatively high (ca. 18 %), and were not strongly affected by co-liquefaction with plastics, with the exception of PE, which decreased bio-crude O content to 10–13 %.

The HHV of bio-crude from co-liquefaction of pistachio hull with plastics was found to be in the range of 32–38 MJ kg^{-1} (Figure 6b). In the presence of PE, the HHV increased from 33.6 MJ kg^{-1} for pure pistachio hull bio-crude to 38.0 and 36.8 Mj/kg for 10 wt.% and 20 wt.% PE blends. However, HHV decreased slightly by 0.6–1.4 % for 20 wt.% blends of PP, PET and nylon. This value was higher than the HHV obtained from pyrolysis pistachio (19.45 MJ kg^{-1}) (Açıkalın et al., 2012). The presence of plastics in biomass hydrothermal liquefaction contribute mostly more increasing in the heating value of bio-crude obtained by reducing the high oxygen content of bio-crude from pure biomass, this resulted can be confirmed by various studies on co-pyrolysis with plastics and biomass (Jung et al., 2010) (Zhou and Yang, 2015) (Aydinli and Caglar, 2010).

Hydrothermal liquefaction as employed in this study is a relatively low-energy technique because it doesn't require the vaporisation of water. Due to specific heat capacity and the low compressibility of water, the energy consumption required to achieve the critical conditions is not excessive, with the completed reaction taking place within 15 minutes. The energy required for hydrothermal liquefaction is less in terms of biomass drying and dewatering processing due to the avoidance of the evaporation step. Therefore, hydrothermal liquefaction processing can lead to high net energy values. This investigation can be confirmed by various studies including (Watson et al., 2019) (Chan et al., 2016) (Yang et al., 2017) (Zhu et al., 2014) (Elliott et al., 2015).

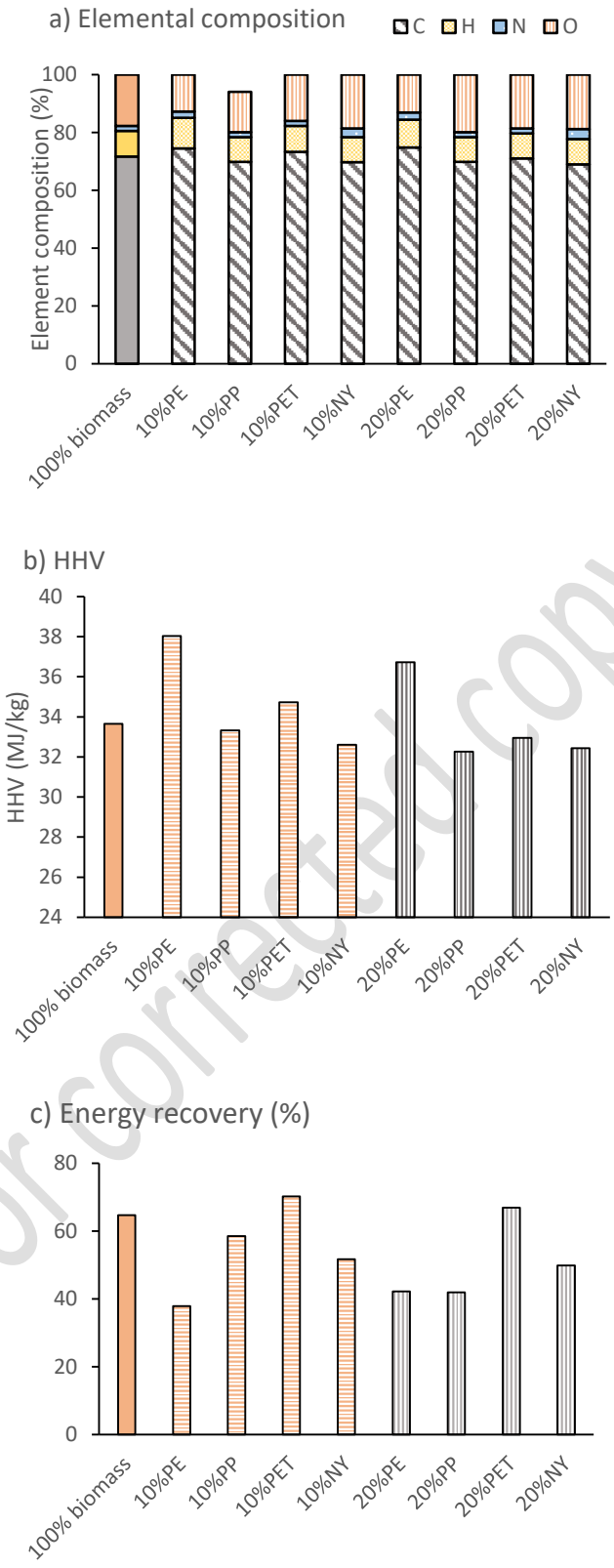

Figure 6 (a) Bio-crude composition from the co-liquefaction of pistachio hulls with 10 wt.% and 20 wt.% PE, PP, PET and NY blend loading, b) bio-crude heating value, and (c) the energy recovery in the bio-crude products from the co-liquefaction of pistachio hulls with PE,PP, PET and NY at 10 wt.% and 20 wt.% blend levels.

In order to determine the effective outcome, the energy in the feedstock is converted into the bio-crude phase product which is a key target of hydrothermal liquefaction products. The energy recovery was calculated based on the bio-crude yield, elemental composition and heating value obtained. Considering the energy recovery (Figure 6c), the highest overall energy recovery was found for 20 wt.% blend PET (70%), this was observed to be similar to bio-crude produced from straw types via pyrolysis (Tröger et al., 2013). Energy recovery was also enhanced compared to the HTL from pure pistachio (60%). In contrast, 10 wt.% blend PE showed the lowest energy conversion (38%), this result is relative to lower bio-crude oil productive of co-liquefaction pistachio with PE.

3.6 Bio-crude chemical composition

In order to investigate the effect of plastics on the bio-crude composition, GC-MS was used to characterise the bio-crudes produced from co-liquefaction of pistachio hull with PP, PE, PE, NY and mixtures of the above. The compounds identified were classified into three categories based on the functional groups: (1) monoaromatics such as benzene, phenol and their derivatives, (2) aliphatic compounds such as cyclopentene and cyclohexene, and (3) oxygenated compounds such as acetic acid-4-methylphenyl ester for example. The majority of compounds identified in each bio-crude were composed predominantly of phenolic compounds – these presumably originate from lignin, which is one of the major components of the pistachio hulls.

GC-MS analysis of the bio-crude from pure pistachio hull showed the presence of phenolic compounds, substituted cyclopentenones, and low levels of 4-methyl,1,2-benzenediol. PET, PP and nylon are more susceptible to degradation than PE – kinetic studies on the decomposition of polyolefins have found that the minimum amount of energy required to activate PP and PE was equal to 243 and 301 kJ mol^{-1}, respectively (Wall et al., 1954). For co-liquefaction with PE, degradation of the polymer chains through a random scission mechanism was expected to form aliphatic hydrocarbons (Pei et al., 2012).

A slight increase in ketone formation was observed in the presence of PE, however, no increase in the abundance of medium- or long-chain aliphatic hydrocarbons was detected as evidence of PE fragmentation (although it is possible that fragmentation products were present, but too large to be soluble).

An unexpected increase in the relative abundance of pyridinol and its derivatives was also observed in the presence of PET, suggesting that PET activates protein decomposition in the pistachio hull biomass. Additionally, the presence of variously substituted benzenediols and phenols may originate from PET decomposition, although terephthalic acid monomer was not observed. Co-liquefaction of biomass with nylon 6 resulted in the appearance of a large peak attributable to monomeric caprolactam in the bio-crude. Caprolactam has previously been shown to depolymerise in aqueous conditions at temperatures as low as 120°C (Brydson, 1999). Caprolactam is soluble in both chloroform and water, so is likely to be distributed between the bio-crude and aqueous phases. A summary of the most abundant compounds in the bio-crudes produced, identified using GC-MS, is presented in the Supporting Information (Table S7).

3.7 Aqueous phase

Co-liquefaction of pistachio hulls with PE, PP and PET in the aqueous phase showed a decreased carbon and nitrogen content (Table 1). The total organic carbon and total nitrogen in the aqueous product phases is distributed very similarly with 16.7 %, 17.5 % and 18.4 % for carbon concentration and 0.87, 0.86 and 0.72 % for nitrogen at a 10 wt.% blend of PE, PP, and PET, respectively. Aqueous phase carbon and nitrogen contents decreased slightly for both 10 wt.% and 20 wt.% blends of PE and PP. In contrast, co-liquefaction with nylon shows increases in both carbon and nitrogen content in the aqueous phase at 20.8 and 31.7 % for 10 wt.% and 20 wt.% nylon blend loading. This observation is predominantly due to the formation of water-soluble caprolactam with the depolymerisation of nylon.

Table 1 Elemental composition of aqueous phases produced from liquefaction of pistachio hulls with plastics

Sample	TOC (g L^{-1})	TN (g L^{-1})
100% biomass	17.9	0.94
10% PE	16.7	0.87
10% PP	17.5	0.86
10% PET	18.4	0.72
10% NY	20.9	1.87
10% Mix	19.7	1.26
20% PE	15.0	0.81
20% PP	15.8	0.78
20% PET	18.6	0.64
20% NY	31.7	3.54
20% Mix	22.2	1.91

3.8 Optimisation of reaction time and heating rate

Although it has previously been shown that bio-crude yields are increased at faster heating rates and shorter reaction times (Hietala et al., 2016; Valdez et al., 2012) (Faeth et al., 2013) (Eboibi et al., 2014), longer reaction times and slower heating may enhance the decomposition of unreactive plastics such as PE and PP under HTL conditions. HTL reactions were therefore carried out using slower heating rates (5.5 °C min^{-1}) to achieve longer reaction times, giving an overall reaction time of 60 min. Longer reaction times did not appear to increase bio-crude production, instead contributing to increasing bio-char and gaseous products (fig. 7), in line with previous studies on biomass liquefaction (Bezergianni et al., 2017; Duan and Savage, 2011). At longer reaction times, bio-crude products can polymerise to give heavier oil fractions and solid phase materials, but long reaction times can also result in hydrocracking of organic compounds into gases, further reducing the bio-crude yields. In terms of bio-crude production, there is no benefit to using reaction times longer than 15 min.

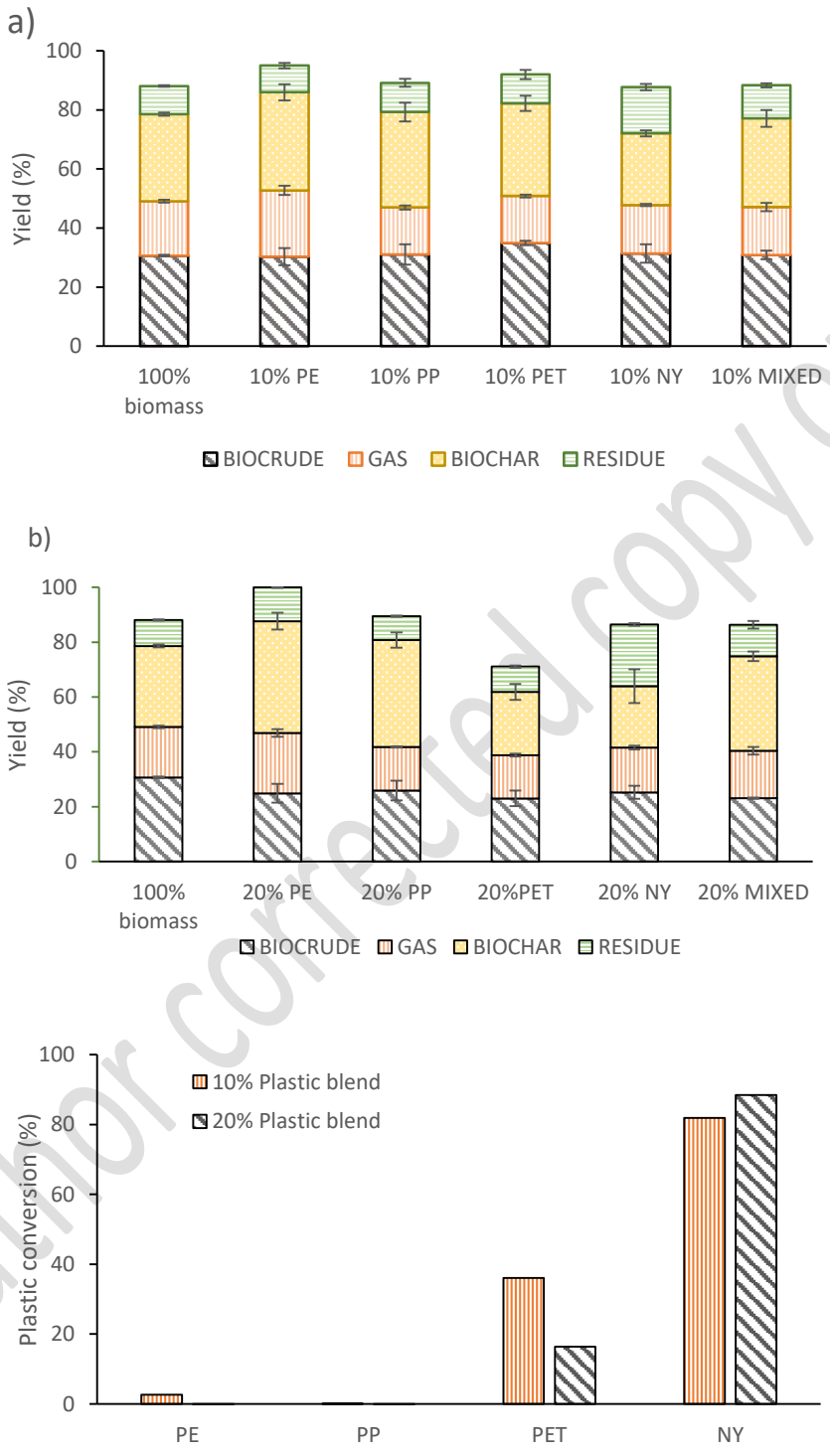

Figure 7 Effect of longer reaction time on products yield where (a) is a plastic loading (PP, PE, PET, NY or mixture) of 10 wt.% (b) is a plastic loading of 20 wt.% (PP, PE, PET, NY or mixture) and c) is the total plastic conversion in the reaction for PE, PP, PET and NY.

Similarly, FT-IR spectroscopy of the bio-char produced from co-liquefaction at slower heating rates suggested that slower heating rates and increasing the reaction time did not facilitate the conversion of plastics. The majority of the peaks observed occurred at identical wavenumbers to those seen in bio-char produced under more severe reaction conditions, with more intense absorbance's suggesting the presence of higher levels of plastics in the bio-char. Notably, C–H adsorption bands were observed at 2924 $cm^{-1}$and 2850 cm^{-1} the PET blends, and at 2935 cm^{-1} and 2868 cm^{-1} for nylon, which were not observed for the bio-chars produced at faster heating rates (see Figure S7 in Supporting Information for all spectra).

The conversion of plastic was calculated using Eqn. 10, as previously. Compared to faster heating rates, HTL carried out at slow heating rates (5.5 °C min^{-1}) gave rise to lower overall conversions of plastics in all cases with the exception of the 10 wt.% NY blend (a slight increase from 74 to 82 % conversion for slow heating rates) and the 20 wt.% NY (a modest increase from 84 to 88 % conversion). This indicates that faster heating rates are preferred for optimising both overall bio-crude yield and plastic conversion.

4. Conclusions

Hydrothermal liquefaction is a highly promising conversion technology for lignocellulosic biomass. In this study the addition of PE, PP, PET and Nylon to the liquefaction of pistachio hulls was investigated, to determine the suitability of co-processing the waste feedstocks together. Promisingly, both PET and nylon-6 were depolymerised under HTL conditions, and in the case of nylon-6, the monomer ϵ-caprolactam was recovered predominantly in the aqueous phase. The polyolefins were much less resistant to decomposition, though what was broken down partitioned into the bio-crude phase and increased the HHV of the bio-crudes substantially. Although co-liquefaction of lignocellulosic residues and contaminated plastic wastes is a potentially elegant means to utilising waste streams for value creation, taking steps to further enhance the conversion of the recalcitrant polyolefins is necessary before plastic waste can become an integral part of a biorefinery.

5. Acknowledgments

The authors would like to acknowledge the Royal Thai Scholarship for funding this study.

References

Açıkalın, K., Karaca, F., Bolat, E., 2012. Pyrolysis of pistachio shell: Effects of pyrolysis conditions and analysis of products. Fuel 95, 169-177.

Akhtar, J., Amin, N.A.S., 2011. A review on process conditions for optimum bio-oil yield in hydrothermal liquefaction of biomass. Renewable and Sustainable Energy Reviews 15, 1615-1624.

Apaydin-Varol, E., Pütün, E., Pütün, A.E., 2007. Slow pyrolysis of pistachio shell. Fuel 86, 1892-1899.

Arturi, K.R., Kucheryavskiy, S., Søgaard, E.G., 2016. Performance of hydrothermal liquefaction (HTL) of biomass by multivariate data analysis. Fuel Processing Technology 150, 94-103.

Association of Plastic Manufacturers Europe, P.t.F., 2016. An analysis of the European plastics production, demand and waste data. European Association of Plastics Recycling and Recovery Organisations (2016), 1-38.

Association of Plastic Manufacturers Europe, P.t.F., 2017. An analysis of European plastics production, demand and waste data, demand and waste data, European Association of Plastics Recycling and Recovery Organisations pp. 1-44.

Aydinli, B., Caglar, A., 2010. The comparison of hazelnut shell co-pyrolysis with polyethylene oxide and previous ultra-high molecular weight polyethylene. Journal of Analytical and Applied Pyrolysis 87, 263-268.

Bezergianni, S., Dimitriadis, A., Faussone, G.-C., Karonis, D., 2017. Alternative Diesel from Waste Plastics. Energies 10, 1750.

Bhada-Tata, D.H.a.P., March 2012 WHAT A WASTE A Global Review of Solid Waste Management, World Bank Urban Development Series.

Bhattacharya, P., Steele, P.H., Hassan, E.B.M., Mitchell, B., Ingram, L., Pittman, C.U., 2009. Wood/plastic copyrolysis in an auger reactor: Chemical and physical analysis of the products. Fuel 88, 1251-1260.

Bi, Z., Zhang, J., Peterson, E., Zhu, Z., Xia, C., Liang, Y., Wiltowski, T., 2017. Biocrude from pretreated sorghum bagasse through catalytic hydrothermal liquefaction. Fuel 188, 112-120.

Biller, P., Sharma, B.K., Kunwar, B., Ross, A.B., 2015. Hydroprocessing of bio-crude from continuous hydrothermal liquefaction of microalgae. Fuel 159, 197-205.

Brydson, J.A., 1999. 18 - Polyamides and Polyimides, in: Brydson, J.A. (Ed.), Plastics Materials (Seventh Edition). Butterworth-Heinemann, Oxford, pp. 478-530.

Burra, K.G., Gupta, A.K., 2018. Kinetics of synergistic effects in co-pyrolysis of biomass with plastic wastes. Applied Energy 220, 408-418.

Cao, B., Sun, Y., Guo, J., Wang, S., Yuan, J., Esakkimuthu, S., Bernard Uzoejinwa, B., Yuan, C., Abomohra, A.E.-F., Qian, L., Liu, L., Li, B., He, Z., Wang, Q., 2019. Synergistic effects of co-pyrolysis of macroalgae and polyvinyl chloride on bio-oil/bio-char properties and transferring regularity of chlorine. Fuel 246, 319-329.

Çepelioğullar, Ö., Pütün, A.E., 2013. Thermal and kinetic behaviors of biomass and plastic wastes in co-pyrolysis. Energy Conversion and Management 75, 263-270.

Chan, Y., Tan, R., Suzana, Y., Lam, H., Quitain, A., 2016. Comparative life cycle assessment (LCA) of bio-oil production from fast pyrolysis and hydrothermal liquefaction of oil palm empty fruit bunch (EFB). Clean Technologies and Environmental Policy 18.

Chen, B., Zhou, D., Zhu, L., 2008. Transitional Adsorption and Partition of Nonpolar and Polar Aromatic Contaminants by Biochars of Pine Needles with Different Pyrolytic Temperatures. Environmental Science & Technology 42, 5137-5143.

Chen, Y., Furmann, A., Mastalerz, M., Schimmelmann, A., 2014. Quantitative analysis of shales by KBr-FTIR and micro-FTIR. Fuel 116, 538-549.

Costanzo, W., Hilten, R., Jena, U., Das, K.C., Kastner, J.R., 2016. Effect of low temperature hydrothermal liquefaction on catalytic hydrodenitrogenation of algae biocrude and model macromolecules. Algal Research 13, 53-68.

Demiral, İ., Atilgan, N.G., Şensöz, S., 2008. PRODUCTION OF BIOFUEL FROM SOFT SHELL OF PISTACHIO (PISTACIA VERA L.). Chemical Engineering Communications 196, 104-115.

Demirbaş, A., 2001. Biomass resource facilities and biomass conversion processing for fuels and chemicals. Energy Conversion and Management 42, 1357-1378.

Demirbas, A., Al-Sasi, B.O., Nizami, A.-S., 2016. Conversion of waste tires to liquid products via sodium carbonate catalytic pyrolysis. Energy Sources, Part A: Recovery, Utilization, and Environmental Effects 38, 2487-2493.
Duan, P., Savage, P.E., 2011. Hydrothermal Liquefaction of a Microalga with Heterogeneous Catalysts. Industrial & Engineering Chemistry Research 50, 52-61.
Eboibi, B.E., Lewis, D.M., Ashman, P.J., Chinnasamy, S., 2014. Effect of operating conditions on yield and quality of biocrude during hydrothermal liquefaction of halophytic microalga Tetraselmis sp. Bioresource Technology 170, 20-29.
Elliott, D.C., Biller, P., Ross, A.B., Schmidt, A.J., Jones, S.B., 2015. Hydrothermal liquefaction of biomass: Developments from batch to continuous process. Bioresource Technology 178, 147-156.
Faeth, J.L., Valdez, P.J., Savage, P.E., 2013. Fast Hydrothermal Liquefaction of Nannochloropsis sp. To Produce Biocrude. Energy & Fuels 27, 1391-1398.
Fekhar, B., Miskolczi, N., Bhaskar, T., Kumar, J., Dhyani, V., 2018. Co-pyrolysis of biomass and plastic wastes: investigation of apparent kinetic parameters and stability of pyrolysis oils. IOP Conference Series: Earth and Environmental Science 154, 012022.
Hietala, D.C., Faeth, J.L., Savage, P.E., 2016. A quantitative kinetic model for the fast and isothermal hydrothermal liquefaction of Nannochloropsis sp. Bioresource Technology 214, 102-111.
Hu, Y., Wang, S., Li, J., Wang, Q., He, Z., Feng, Y., Abomohra, A.E.-F., Afonaa-Mensah, S., Hui, C., 2018. Co-pyrolysis and co-hydrothermal liquefaction of seaweeds and rice husk: Comparative study towards enhanced biofuel production. Journal of Analytical and Applied Pyrolysis 129, 162-170.
Jakab, E., Várhegyi, G., Faix, O., 2000. Thermal decomposition of polypropylene in the presence of wood-derived materials. Journal of Analytical and Applied Pyrolysis 56, 273-285.
Jongwon Kim, S.B.L.C.B.M.B.A.A., 1999. Coliquefaction of Coal and Black Liquor to Environmentally Acceptable Liquid Fuels. Energy Sources 21, 839-847.
Jung, S.-H., Cho, M.-H., Kang, B.-S., Kim, J.-S., 2010. Pyrolysis of a fraction of waste polypropylene and polyethylene for the recovery of BTX aromatics using a fluidized bed reactor. Fuel Processing Technology 91, 277-284.
Karaca, F., Bolat, E., 2000. Coprocessing of a Turkish lignite with a cellulosic waste material: 1. The effect of coprocessing on liquefaction yields at different reaction temperatures. Fuel Processing Technology 64, 47-55.
Konsolakis, M., Kaklidis, N., Marnellos, G.E., Zaharaki, D., Komnitsas, K., 2015. Assessment of biochar as feedstock in a direct carbon solid oxide fuel cell. RSC Advances 5, 73399-73409.
Kookana, R., K. Sarmah, A., Van Zwieten, L., Van Krull, E., Singh, B., 2011. Biochar Application to Soil: Agronomic and Environmental Benefits and Unintended Consequences. Advances in Agronomy 112, 103-143.
Lao, W., li, G., 2014. Quantitative Analysis of Biomass in Three Types of Wood-Plastic Composites by FTIR Spectroscopy. Bioresources 9(4), 6073-6086.
Liu, Z., Zhang, F.-S., Wu, J., 2010. Characterization and application of chars produced from pinewood pyrolysis and hydrothermal treatment. Fuel 89, 510-514.
Lua, A.C., Yang, T., 2004. Effect of activation temperature on the textural and chemical properties of potassium hydroxide activated carbon prepared from pistachio-nut shell. Journal of Colloid and Interface Science 274, 594-601.
Nazari, L., Yuan, Z., Souzanchi, S., Ray, M.B., Xu, C., 2015. Hydrothermal liquefaction of woody biomass in hot-compressed water: Catalyst screening and comprehensive characterization of bio-crude oils. Fuel 162, 74-83.
Pandey, K.K., Pitman, A.J., 2004. Examination of the lignin content in a softwood and a hardwood decayed by a brown-rot fungus with the acetyl bromide method and Fourier transform infrared spectroscopy. Journal of Polymer Science Part A: Polymer Chemistry 42, 2340-2346.
Pedersen, T.H., Grigoras, I.F., Hoffmann, J., Toor, S.S., Daraban, I.M., Jensen, C.U., Iversen, S.B., Madsen, R.B., Glasius, M., Arturi, K.R., Nielsen, R.P., Søgaard, E.G., Rosendahl, L.A., 2016. Continuous hydrothermal co-liquefaction of aspen wood and glycerol with water phase recirculation. Applied Energy 162, 1034-1041.

Pei, X., Yuan, X., Zeng, G., Huang, H., Wang, J., Li, H., Zhu, H., 2012. Co-liquefaction of microalgae and synthetic polymer mixture in sub- and supercritical ethanol. Fuel Processing Technology 93, 35-44.
Peterson, A.A., Vogel, F., Lachance, R.P., Fröling, M., Antal, J.M.J., Tester, J.W., 2008. Thermochemical biofuel production in hydrothermal media: A review of sub- and supercritical water technologies. Energy & Environmental Science 1.
Pütün, A.E., Özbay, N., Apaydın Varol, E., Uzun, B.B., Ateş, F., 2007. Rapid and slow pyrolysis of pistachio shell: effect of pyrolysis conditions on the product yields and characterization of the liquid product. International Journal of Energy Research 31, 506-514.
Qian, K., Ajay, K., Patil, K., Bellmer, D., Wang, D., Yuan, W., Huhnke, R., 2013. Effects of Biomass Feedstocks and Gasification Conditions on the Physiochemical Properties of Char. Energies 6, 3972-3986.
Raikova, S., Knowles, T.D.J., Allen, M.J., Chuck, C.J., 2019. Co-liquefaction of Macroalgae with Common Marine Plastic Pollutants. ACS Sustainable Chemistry & Engineering 7, 6769-6781.
Raikova, S., Smith-Baedorf, H., Bransgrove, R., Barlow, O., Santomauro, F., Wagner, J.L., Allen, M.J., Bryan, C.G., Sapsford, D., Chuck, C.J., 2016. Assessing hydrothermal liquefaction for the production of bio-oil and enhanced metal recovery from microalgae cultivated on acid mine drainage. Fuel Processing Technology 142, 219-227.
Shui, H., Jiang, Q., Cai, Z., Wang, Z., Lei, Z., Ren, S., Pan, C., Li, H., 2013. Co-liquefaction of rice straw and coal using different catalysts. Fuel 109, 9-13.
Shui, H., Shan, C., Cai, Z., Wang, Z., Lei, Z., Ren, S., Pan, C., Li, H., 2011. Co-liquefaction behavior of a sub-bituminous coal and sawdust. Energy 36, 6645-6650.
Sørum, L., Grønli, M.G., Hustad, J.E., 2001. Pyrolysis characteristics and kinetics of municipal solid wastes. Fuel 80, 1217-1227.
Stark, N.M., Matuana, L.M., 2007. Characterization of weathered wood–plastic composite surfaces using FTIR spectroscopy, contact angle, and XPS. Polymer Degradation and Stability 92, 1883-1890.
Taghizadeh-Alisaraei, A., Assar, H.A., Ghobadian, B., Motevali, A., 2017. Potential of biofuel production from pistachio waste in Iran. Renewable and Sustainable Energy Reviews 72, 510-522.
Taghizadeh, A., Rad-Moghadam, K., 2018. Green fabrication of Cu/pistachio shell nanocomposite using Pistacia Vera L. hull: An efficient catalyst for expedient reduction of 4-nitrophenol and organic dyes. Journal of Cleaner Production 198, 1105-1119.
Tan, X., Liu, Y., Zeng, G., Wang, X., Hu, X., Gu, Y., Yang, Z., 2015. Application of biochar for the removal of pollutants from aqueous solutions. Chemosphere 125, 70-85.
Tekin, K., Karagöz, S., Bektaş, S., 2014. A review of hydrothermal biomass processing. Renewable and Sustainable Energy Reviews 40, 673-687.
Tews, I.J., Zhu, Y., Drennan, C., Elliott, D.C., Snowden-Swan, L.J., Onarheim, K., Solantausta, Y., Beckman, D., 2014. Biomass Direct Liquefaction Options. TechnoEconomic and Life Cycle Assessment. ; Pacific Northwest National Lab. (PNNL), Richland, WA (United States), p. Medium: ED; Size: PDFN.
Tröger, N., Richter, D., Stahl, R., 2013. Effect of feedstock composition on product yields and energy recovery rates of fast pyrolysis products from different straw types. Journal of Analytical and Applied Pyrolysis 100, 158-165.
Uzoejinwa, B.B., He, X., Wang, S., El-Fatah Abomohra, A., Hu, Y., Wang, Q., 2018. Co-pyrolysis of biomass and waste plastics as a thermochemical conversion technology for high-grade biofuel production: Recent progress and future directions elsewhere worldwide. Energy Conversion and Management 163, 468-492.
Valdez, P.J., Nelson, M.C., Wang, H.Y., Lin, X.N., Savage, P.E., 2012. Hydrothermal liquefaction of Nannochloropsis sp.: Systematic study of process variables and analysis of the product fractions. Biomass and Bioenergy 46, 317-331.
Van Krevelen, D.W., 1950. Graphical-statistical method for the study of structure and reaction processes of coal. Fuel 29, 269-284.
Wall, L.A., Madorsky, S.L., Brown, D.W., Straus, S., Simha, R., 1954. The Depolymerization of Polymethylene and Polyethylene. Journal of the American Chemical Society 76, 3430-3437.
Wang, B., Huang, Y., Zhang, J., 2014. Hydrothermal liquefaction of lignite, wheat straw and plastic waste in sub-critical water for oil: Product distribution. Journal of Analytical and Applied Pyrolysis 110, 382-389.

Wang, S.-H., Griffiths, P.R., 1985. Resolution enhancement of diffuse reflectance i.r. spectra of coals by Fourier self-deconvolution: 1. C-H stretching and bending modes. Fuel 64, 229-236.
Wang, X., Zhou, W., Liang, G., Song, D., Zhang, X., 2015. Characteristics of maize biochar with different pyrolysis temperatures and its effects on organic carbon, nitrogen and enzymatic activities after addition to fluvo-aquic soil. Science of The Total Environment 538, 137-144.
Watson, J., Lu, J., de Souza, R., Si, B., Zhang, Y., Liu, Z., 2019. Effects of the extraction solvents in hydrothermal liquefaction processes: Biocrude oil quality and energy conversion efficiency. Energy 167, 189-197.
Wong, S.L., Ngadi, N., Abdullah, T.A.T., Inuwa, I.M., 2015. Current state and future prospects of plastic waste as source of fuel: A review. Renewable and Sustainable Energy Reviews 50, 1167-1180.
Wu, X., Liang, J., Wu, Y., Hu, H., Huang, S., Wu, K., 2017. Co-liquefaction of microalgae and polypropylene in sub-/super-critical water. RSC Advances 7, 13768-13776.
Xiu, S., Shahbazi, A., Shirley, V., Cheng, D., 2010. Hydrothermal pyrolysis of swine manure to bio-oil: Effects of operating parameters on products yield and characterization of bio-oil. Journal of Analytical and Applied Pyrolysis 88, 73-79.
Yang, C., Wu, J., Deng, Z., Zhang, B., Cui, C., Ding, Y., 2017. A Comparison of Energy Consumption in Hydrothermal Liquefaction and Pyrolysis of Microalgae. Trends in Renewable Energy 3, 76-85.
Zhou, C., Yang, W., 2015. Effect of heat transfer model on the prediction of refuse-derived fuel pyrolysis process. Fuel 142, 46-57.
Zhu, Y., Biddy, M.J., Jones, S.B., Elliott, D.C., Schmidt, A.J., 2014. Techno-Economic Analysis of Liquid Fuel Production from Woody Biomass via Hydrothermal Liquefaction (HTL) and Upgrading. Applied Energy, 129:384-394, Medium: X.

Co-processing of common plastics with pistachio hulls via hydrothermal liquefaction

Supporting Information

1.1 Properties of pistachio hull feedstock

Table S1 – Properties of pistachio hull feedstock

Properties	Result	Method
Moisture	14.31 wt.%	ASTM E1755
Ash	4.24 wt. %	ASTM E1755
Volatile Matter	70.09 wt. %	ASTM E1755
Fixed Carbon	11.35 wt. %	ASTME1755
Carbon	41.22 wt. %	ASTM D5291
Sulfur	0.13 wt. %	ASTM E3177
Hydrogen	6.98 wt. %	ASTM D5291
Nitrogen	1.34 wt. %	ASTM D5291
Oxygen by Difference	46.08 wt. %	ASTM D5291
Lower Heating Value	17.45 MJ kg^{-1}	ASTM E711
Higher Heating Value	18.97 MJ kg^{-1}	ASTM E711

1.2 Feedstock elemental compositions

The elemental compositions of the plastic feedstocks is presented in Table S2. PE and PP had the highest energy content (measured as HHV) of all five feedstocks due to their high carbon and hydrogen content. PET possessed the lowest energy content as a result of its high oxygen content; the HHV of pistachio hull biomass was somewhat higher. Nylon contained high levels of nitrogen, and had an HHV of 28.6 MJ kg^{-1}. The initial energy contents and elemental compositions of the feedstocks will have an impact on the yields and compositions of bio-crudes produced by HTL, and high feedstock oxygen and nitrogen content can pose a significant challenge – O- and N-rich bio-crudes would require significant further upgrading to create usable fuels.

Table S2 – Elemental composition and HHV of plastics

Element Analysis (%)	C	H	O	N	HHV (MJ kg^{-1})
Pistachio hull	49.3	6.8	46.1	1.78	17.5
PE	84.9	12.2	2.9	<0.1	45.6
PP	85.1	13.3	1.5	<0.1	47.4
PET	43.7	4.0	52.0	0.41	11.2
NY	60.8	8.1	19.1	12.0	28.6

1.3 Calibration curves for quantification of unreacted plastics in bio-char using FTIR

The FTIR and resulting calibration curves for quantification of unreacted plastics in bio-char using FTIR are presented below. The quantity of unreacted plastic in bio-char samples was used to calculate, by extension, the percentage of plastic feed undergoing conversion to other products (bio-crude, aqueous or gaseous). This method makes a number of assumptions; in particular, that the bio-char formed from pistachio hull in the presence of plastics does not undergo any changes in composition, apart from containing unreacted plastics, and that any plastics in the bio-char are entirely unchanged. These assumptions mean that the method must be treated cautiously as a semi-quantitative approximation. In some cases, conversions <0% were observed; these have been approximated as 0% after accounting for error.

1.3.1 Polyethylene in bio-char

Figure S1a shows infrared spectra of eight samples of pure pistachio hull bio-char blended with unreacted PE at concentrations within the range 0–100 wt.%. The strong absorption band at 898 cm^{-1} was taken as a representative peak for pistachio hull bio-char. The band at 2917 cm^{-1} was chosen as a reference for PE. The relative intensities of the characteristic bands were used as indicators of PE content in bio-chars. Peak intensity ratios (PIR) were calculated for each blend, and used to create a calibration curve, shown in **Figure S1b**. A high coefficient of determination (R^2) was obtained for the calibration curve (0.9538). PIRs were then calculated from the FTIR spectra of the bio-char resulting from HTL of pistachio hull/polyethylene at 10 wt.% and 20 wt.% blends to quantify unreacted PE.

The calculated values for unreacted PE in co-liquefaction chars are summarised in **Table S2**. For the reactions carried out at a fast heating rate, the content of unreacted PE in the bio-char was calculated as 26 % and 60 % for 10 wt.% and 20 wt.% PE blend levels, respectively; 31 % and 63

% unreacted PE were detected in the bio-char for slow heating rates for 10 wt.% and 20 wt.% PE blends**.**

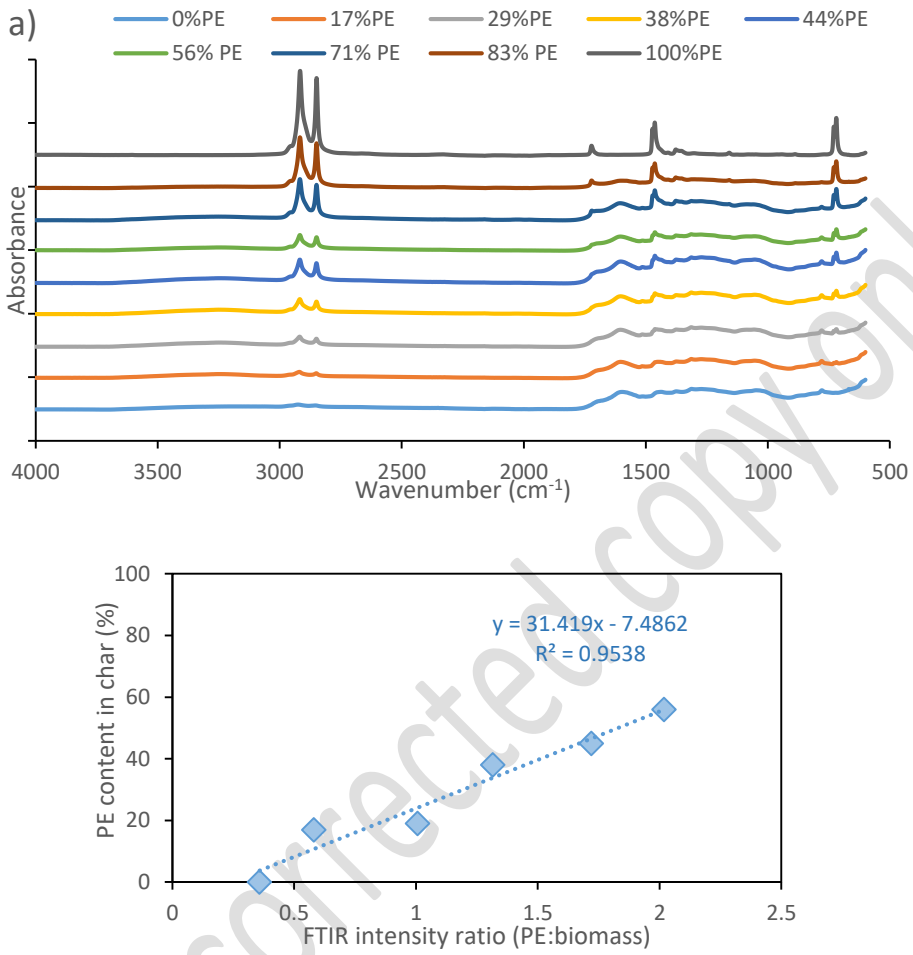

Figure S1 – (a) FTIR spectra of pistachio hulls bio-char with different polyethylene contents, and (b) peak intensity ratio calibration curve for polyethylene content in pistachio hull bio-char.

Table S3 – Calculated percentage concentrations of unreacted polyethylene in bio-char from co-liquefaction of pistachio hull with PE.

	PE	Pistachio hull bio-char	PIR	Predictive equation	R^2	Unreacted PE in char (%)
	2917 cm^{-1}	**898 cm^{-1}**	**2917:898**	y = 31.419 + 7.4862	0.9538	
Fast heating rate						
10%PE	0.0434	0.0408	1.0640			26
20%PE	0.0582	0.0270	2.1578			60
Slow heating rate						
10%PE	0.037521	0.030315	1.237711			31
20%PE	0.097836	0.042746	2.288778			64

1.3.2 Polypropylene in bio-char

As previously, the absorbance band at 898 cm^{-1} was used as the indicative band for pistachio hull bio-char, whilst the strong peak at 2914 cm^{-1} was used to represent PP (**Figure S2a**). However, two calibration curves were created in this case for the blend level ranges 0–38 % PP in bio-char, and 38–100 % PP. Coefficients of determination of <0.85 were obtained in both cases. Unreacted polypropylene in bio-char was calculated to make up 37 % and 50 % of the total bio-char for the faster heating rate, and 55 % and 56 % for the slower heating rate for co-liquefaction of 10 wt.% and 20 wt.% PP blends in biomass, respectively (**Figure S2b**).

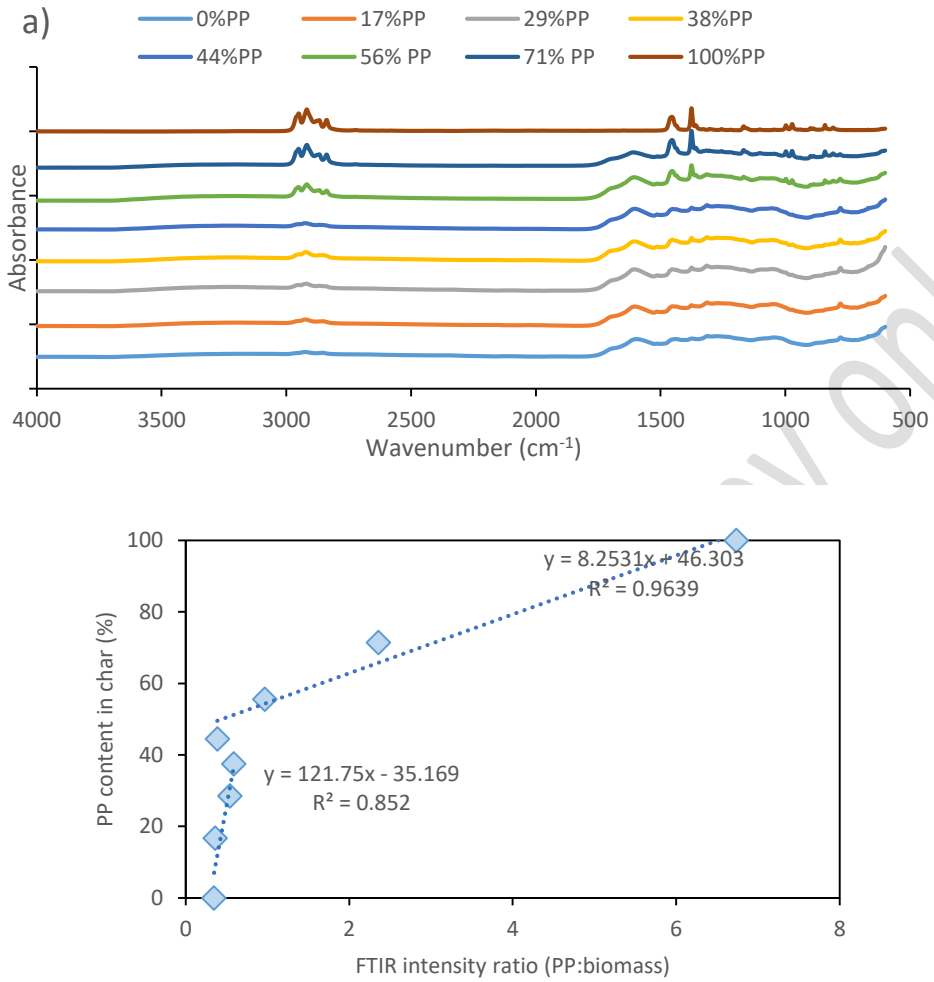

Figure S2 – (a) FTIR spectra of pistachio hull bio-char with different polypropylene contents and (b) peak ratio calibration curve for polypropylene in pistachio bio-char.

Table S4 – Calculated percentage concentrations of unreacted polypropylene in bio-char from co-liquefaction of pistachio hull with PP.

	PP	Pistachio hull bio-char	PIR	Predictive equation	R2	Unreacted PP in char (%)
	2914 cm^{-1}	**898 cm^{-1}**	**2914:898**	0–37 % PP: y = 121.75x – 35.169 37–100 % PP: y = 8.2531 + 46.303	0.852 0.9636	
Fast heating rate						
10%PP	0.017744	0.029852	0.594401			37
20%PP	0.019885	0.028489	0.698003			50
Slow heating rate						
10%PP	0.040715	0.038076	1.06929472			55
20%PP	0.06919	0.057573	1.20177729			56

1.3.3 Polyethylene terephthalate in bio-char

For co-liquefaction of PET/biomass, difficulties in homogenising the calibration samples meant that a somewhat lower coefficient of determination was obtained for the calibration curve (R^2 = 0.81). A number of absorbances were examined, and the calibration curve for PET/biomass bio-char was established using the peak in the region 898 cm^{-1} as the reference for pistachio bio-char. The strongest absorption band observed for PET occurred at 726 cm^{-1} (*assigned* to the aromatic ring) (**Figure S3a**).

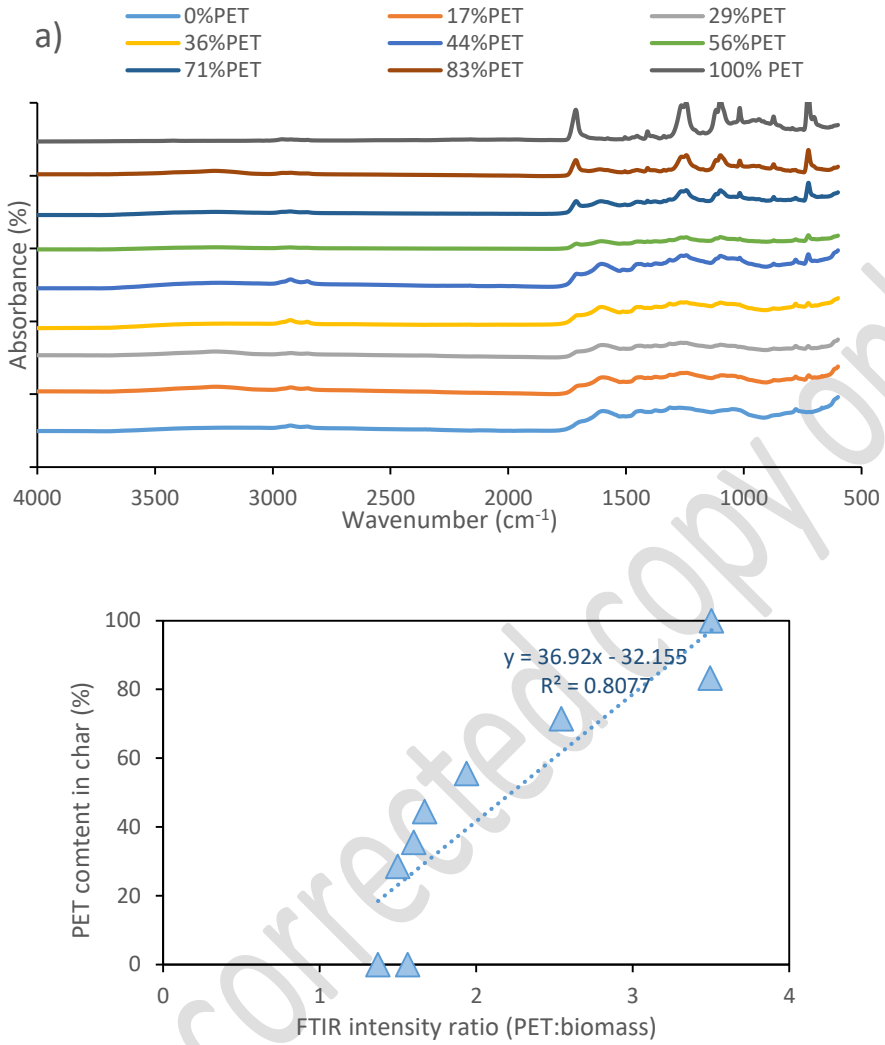

Figure S3 (a) FTIR spectra of pistachio hulls bio-char with different polypropylene contents, and (b) peak ratio calibration curve for polyethylene terephthalate in pistachio bio-char.

Table S5 – Calculated percentage concentrations of unreacted polyethylene terephthalate in bio-char from co-liquefaction of pistachio hull with PET.

	PET	Pistachio hull bio-char	PIR	Predictive equation	R^2	Unreacted PET in char (%)
	726 cm^{-1}	**898 cm^{-1}**	**726:898**	y = 36.92x – 32.155	0.8077	
Fast heating rate						
10%PET	0.020853	0.016007	1.302738			22
20%PET	0.030037	0.048166	1.603535			32
Slow heating rate						
10%PET	0.070744	0.053181	1.330259			23
20%PET	0.08616	0.042746	2.01563			46

1.3.4 Nylon in bio-char

For nylon, the representative absorbance band was selected as 1534 cm^{-1}, whilst 898 cm^{-1} was used for pistachio hull bio-char. For all the calibration curves, the coefficient of determination (R^2) exceeded 0.98. The results showed that the content of unreacted nylon in co-liquefaction bio-char was around 11 % and 9 % for fast heating rates, and 7 % and 11 % for slow heating rate, for 10 wt.% and 20 wt.% nylon/pistachio blends respectively. This signifies a substantially higher overall conversion of nylon under HTL conditions relative to the other plastic feedstocks examined.

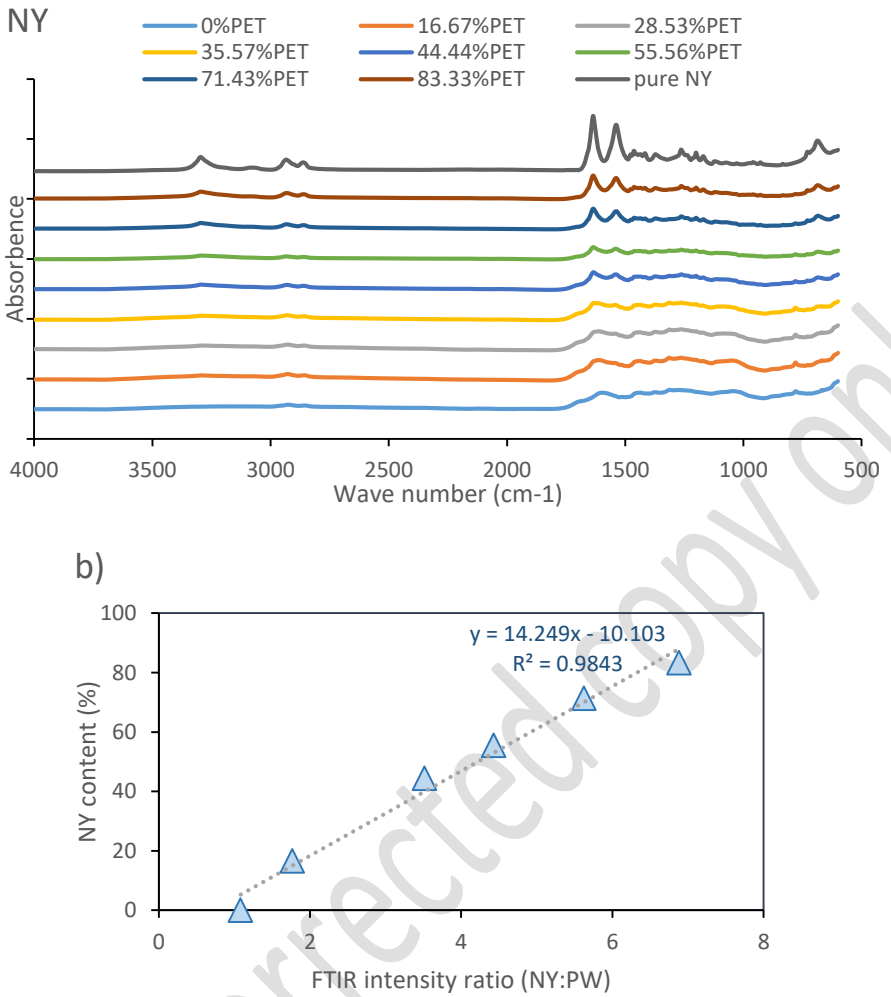

Figure S4 – (a) FTIR spectra of pistachio hulls with different nylon contents, and (b) Peak ratio calibration curve for nylon in pistachio bio-char.

Table S6 – Calculated percentage concentrations of unreacted nylon in bio-char from co-liquefaction of pistachio hull with NY.

	NY	**Pistachio hull bio-char**	**PIR**	**Predictive equation**	**R^2**	**Unreacted NY in char (%)**
	1534 cm^{-1}	**898 cm^{-1}**	**1534:898**	y = 14.249x – 10.103	0.9843	
Fast heating rate						
10%NY	0.026013	0.017696	1.469988			11
20%NY	0.021795	0.015897	1.371049			9
Slow heating rate						
10%NY	0.045761	0.038718	1.181887			7
20%NY	0.087956	0.058233	1.510419			11

1.4 GC/MS analysis of bio-crudes

The identities of notable compounds in bio-crudes from co-liquefaction of biomass with plastics, identified using GC/MS, are presented in Table S7 below. Compounds were not quantified; shaded cells indicate the presence of a compound.

Table S7 – Identities of notable compounds in bio-crude products from co-liquefaction of pistachio hull with 20 wt.% plastics (fast heating rate).

Compound identified	100 % biomass	20 wt.% PE	20 wt.% PP	20 wt.% PET	20 wt.% NY	20 wt.% mix
	Relative abundance					
Styrene			■			■
Butanoic acid, 4-hydroxy-	■	■	■			
Cyclohexene, 4-ethenyl-					■	
2-Cyclohexen-1-one, 4,4,6-trimethyl-			■			
Phenol	■	■	■	■	■	■
.alpha.-Methylstyrene		■	■	■	■	■
Benzaldehyde			■		■	■
Butyrolactone						■
Hexylene glycol			■			■
2-Cyclopenten-1-one, 2-methyl				■	■	■
2-Cyclopenten-1-one, 3-methyl				■	■	■
2-Cyclopenten-1-one, 3-ethyl	■	■	■	■		
2-Cyclopenten-1-one, 2,3-dimethyl			■	■	■	■
Phenol, 2-methyl					■	■
Phenol, 2-methoxy-	■	■	■	■		■
Benzyl alcohol			■		■	■
Phenol, 3-methyl			■			
Acetophenone					■	■
p-Cresol	■	■	■	■	■	■
2-Cyclopenten-1-one, 3-ethyl-	■		■		■	■
Mequinol	■				■	
3-Pyridinol	■	■	■	■	■	
4-Pyridinol					■	■
4-Pyridinemethanol		■		■		
2(1H)-Pyridinone, 3-methyl-				■		
3-Pyridinol, 6-methyl-		■		■		■
1-Cyclohexene-1-carboxylic acid		■		■		
1,2-Cyclooctadiene				■		
Hydroquinone				■		
Benzoic acid		■				
Cyclooctane, 1,2-dimethyl-					■	■
Phenol, 4-ethyl-	■	■	■	■	■	■

Compound identified	100 % biomass	20 wt.% PE	20 wt.% PP	20 wt.% PET	20 wt.% NY	20 wt.% mix
	Relative abundance					
Tetradecane						
4-Tetradecene, (E)-						
Decane, 6-ethyl-2-methyl-						
Cresol						
Catechol						
Caprolactam						
1,2-Benzenediol, 4-methyl-						
Phenol, 2,6-dimethoxy-						
Phenol, 4-ethyl-2-methoxy-						
Diphenyl sulfone						
Benzene, (ethylthio)-						
1,2-Benzenediol, 3-methyl						
1,2-Benzenediol, 3-methoxy						
1,4-Benzenediol, 2-methyl-						
Benzene, 1,2,4-trimethyl-5-(1-methylethyl)-						
Phenol, 2,6-dimethoxy-						
Phenol, 2-methoxy-4-propyl-						
Phenol, 4-methyl-2-nitro-						
4-Ethylthiophenol						
Ethanone, 1-(2-hydroxyphenyl)-						
Phenol, 3-pentadecyl-						
1-Hexadecyne						

1.5 FTIR of bio-chars obtained at from slow HTL (60 min)

Figure S7 – FTIR of pure plastics and bio-char from slow (60 min) HTL of pistachio hull with *(a) polyethylene, (b) polypropylene,* (c) polyethylene terephthalate, and (d) nylon 6.

1.6 Biomass proximate analysis

Table S8 Analysis of pistachio hull feedstock

Analyses	***Pistachio hull***
Proximate (wt.%)	
Total ash	9.4
Water Extractable Others	15.6
Biomass composition (wt.%)	
Lignin	26.6
Glucan	13.6
Xylan	5.0
Galactan	2.8
Arabinan	4.8
Fructan	0.0
Acetyl	1.4
Elemental (wt.%)	
C	41.22
H	6.98
N	1.34
O	46.08